Michiel Meeuwissen

Photo conductive properties of Poly-LED-devices

Universiteit Utrecht

PHILIPS

Author Michiel Meeuwissen

Supervisor Paul Blom

Title Photo conductive properties of Poly-LED-devices

Abstract

This research was originally intended to measure the so called barrier-height for electrons moving from a metal into PPV-polymers used in polymeric LED-devices. This was tried with an optical technique called internal photo emission, in which the increase of current as function of the photon-energy of the illumination is measured.

It became however clear that the current is influenced by the illumination indeed, but that it cannot be caused by an improved injection of electrons on the contact. From current-voltage measurements on polymer-LEDs it is known that a Ca contact is a better electron emitter than an In-contact due to its lower work function. The photo-current, however, does not depend on the work-function of the contact metals used. This clearly indicates that the observed photocurrent does not originate from improved injection of electrons.

The current-voltage characteristics of ITO/PPV/Au however, in which only holes will flow, are dominated by space charge limited conduction without empty traps (localized electronic states in the band-gap). It is concluded that the observed photo-conduction (well below the band-gap of the material) was caused by unfilling of full hole traps of the polymer itself, which without illumination do not contribute to the current. As demonstrated with a numerical simulation this indeed can increase current. Intuitively it can be seen as an increase of effective mobility, the conduction of holes is helped by the continuous presence of extra holes.

Keywords

Poly LED, PPV, Internal Photo Emission, photo-conductivity, T_{12}

Samenvatting

Dit onderzoek was oorspronkelijk begonnen om de zogenaamde barrierehoogte voor electronen die van een metaal naar een PPV-polymeer bewegen, te meten. Deze metaal/polymeer interfaces worden gebruikt in licht gevende diodes (waarin het polymeer het actieve element is). Het was de bedoeling om deze barrierehoogte te bepalen door middel van een optische techniek, interne fotoemissie, waarbij de stroom wordt gemeten als een functie van de energie van de fotonen waarmee het sample wordt belicht.

Het werd in de loop van het onderzoek duidelijk dat de stroom inderdaad wordt beïnvloed door de belichting maar dat dit niet kan komen doordat de electronen op het contact beter injecteren. Uit IV-metingen is namelijk gebleken dat een Ca-contact beter electronen injecteerd dat een In-contact, omdat Ca een lagere werk-functie heeft. De foto-stroom hang echter niet af van de werk-functie van het metaal dat als contact wordt gebruikt.

In ITO/PPV/Au-samples stromen alleen gaten en de IV-curves kunnen beschreven worden met een ruimteladingsbegrensde stroom welke niet word gehinderd door (lege) traps (gelocaliseerde electronische toestanden in de band-gap). De conclusie is dat de gemeten foto-stroom (bij fotonenergieën kleiner dan de bandafstand) is veroorzaakt doordat er volle gatentraps in het polymeer zijn, die worden leeggemaakt met het licht. De gaten worden dan als het ware wat mobieler, doordat er steeds wat gaten zijn uit de traps die helpen aan de geleiding. Dat dit mogelijk is, was gedemonstreerd met behulp van een numeriek computer programma.

Contents

Chapter 1

Introduction

LED devices are nowadays very common in daily life. The active material used in these LED's is normally an inorganic one, such as $GaAs_{1-x}P_x$. These materials are too expensive for application in large-area displays.

In 1990 it was discovered that certain polymers can also be used as the active element in LEDs [13]. Polymers have advantages, above inorganic materials: They are cheaper and have promising mechanical properties (The idea of the *flexible* LED soon rised). Large areas of polymer film can be produced quite easily.

The active polymers, used in these devices, are poly(p-phenylene vinylene) (PPV) and some related polymers. These are so called π-conjugated, indicating the alternating double-single-bonds in its structure formula. By changing the structure of the polymer somewhat, different color LEDs can be obtained. The polymer OC_1C_{10} -PPV, which was used, emits orange light, poly (p-phenylene) blue and ordinary PPV emits yellow-green light. Hopes are that polyLEDs can be used in color LED-displays and even in full-color large-area display such as a computer monitor.

Another advantage of LED-displays, above the also very promising LCD-displays, is that they give light, rather then reflect it. This is also a main disadvantage, because it means that a poly-LED-device dissipates a lot of energy, making it less attractive for portable applications. The efficiency, the brightness per dissipated power, should be maximized therefore. This will also minimize heat production, giving a better lifetime.

A major problem in polymer-LEDs is their short operating lifetimes, which decreases with brightness level. A brightness level of 100 Cd/m^2 (comparable to a computer monitor) at 3V for about 100 hours is typical now.

The light-emission is caused by recombination of electrons and holes. It is expected that most of these recombinations are non-radiative (emitting phonons), thus worsening the efficiency of the devices. The polymer should contain as few as possible non-radiative recombinations sites.

The LED device characteristics are assumed to be dominated by the injection of electrons and holes in the polymer. Parker [55] indicated that the injection is determined by Fowler-Nordheim tunneling through the barriers on the metal-polymer interface.

As a result the electron injection contact should be a low-function metal such as calcium,

the hole injecting contact on the other hand a high work-function transparent (the formed photons must be able to escape the device!) metal. ITO (indium-tin-oxide) was used for this contact. Electron and hole injection rates must be approximately equally high, so minimizing the number of carriers traveling through the polymer without recombining at all, decreasing the efficiency of the device.

Thus important parameters in a device are the 'barrier heights' at the interfaces between Ca and the polymer, and between ITO and the polymer. This determines the injection-rate of respectively electrons and holes. Therefore it was intended to measure these barrier heights by an optical technique called commonly IPE (internal photo emission). This technique is non-destructive, and relatively easy applicable to all sorts of polymer/metal interfaces.

This technique consist of illuminating the Ca(or another metal)/polymer interface with infra-red light, giving rise to hot electrons and holes in the metal. These can be sufficiently energetic to overcome the barrier at the interface. The injection rate on the illuminated contact is thus increased and an additional current will flow. From the photon energy dependency of this photo-injection current the barrier height can be derived.

During our investigations it appeared that these barrier heights are very small, therefore becoming very difficult to measure and irrelevant, because the current is mainly determined by the conductive properties of the polymer itself. In our experiments the incident light not only excites the electrons or holes in the metal but also the polymer itself. The observed photo-current, which arises from the polymer, not from the contacts, is not due to 'intrinsic' photo-conduction, since the the photon energy was smaller than the bandgap (This effect was to be seen at higher photon energies (> 2 eV)). A main topic of this report therefore has become the description and explanation of this phenomenon.

Similar experiments are performed on inorganic thiophene-Schottky-diodes and is added as a modest contribution and comparison to the measurements done at the PPV-samples.

For a description of the setup of this report referred is to the table of contents.

Chapter 2

Theory

This chapter will start with a few sections concerning the 'band structure' associated with a polymer LED followed by a description of the existing ideas about the conductive polymers. Then the theory necessary for understanding the so called 'internal photo-emission' will be dealt with, followed by a treatise on the photo-conductive properties of the polymer itself.

Goal of the research program this work was done in, is to construct a well working polymer-LED device. But not all studied objects are really light emitting, because are purposely not constructed so. Therefore it is more correct to simply speak of a 'sample' in stead of 'polymer LED', and will be done so.

2.1 Conducting polymers

The polymers under study are so called π-conjugated polymers. These are 'conducting' polymers, however with a very low mobility. The polymers are often described in terms of a semiconductor band model or an exciton model [59]. In the exciton model the polymer is regarded as a set of molecules. An exciton is then an excited state of such a molecule. In the semiconductor band model, an exciton is an electron-hole pair, in which the electron and hole eventually have a lower energy then they would have in the conduction and valence band (polaron).

2.1.1 Origin of the band-structure

A polymer can be seen as a one dimensional semiconductor, while the conduction is along the one dimensional chains. A metallic polymer would consist of a just single bond backbone on which the extra electrons can conduct. It can then be seen as a one dimensional metal with a half filled conduction band. Peierls theorem (see e.g. [32, 58]) states that a mono-atomic one-dimensional metal with a half-filled band is unstable. Electron-phonon interactions will cause a lattice distortion, the unit cell will be doubled and an energy gap will occur at the Fermi-level. Electrons below the Fermi-level will be lowered in energy. This lattice distortion is of course nothing but the arising of double bonds, which are

shorter than single bonds (doubling of unit cell), which holds the electrons from conducting.

How the Peierls transition changes the band structure of a one-dimensional metal and the corresponding change in the molecular structure formula of a conjugated polymer is schematicly shown in figure 2.1.

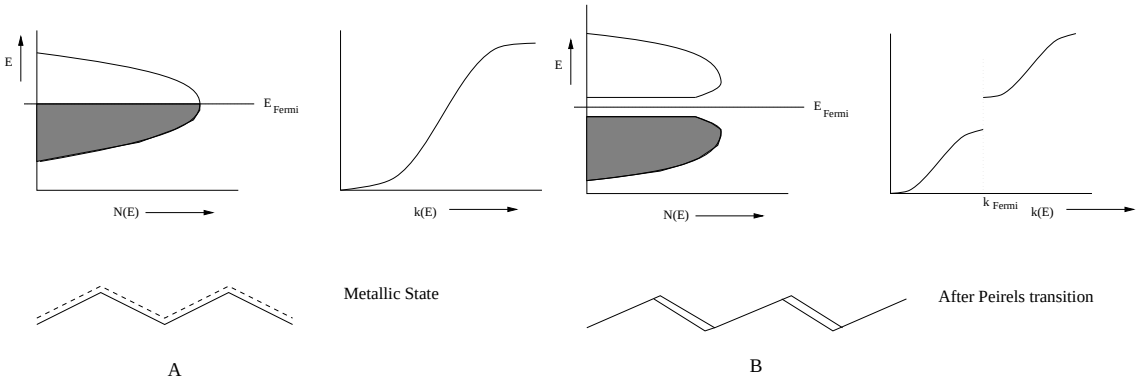

Figure 2.1: Schematic view of the changes in the density of electronic states,in the electron dispersion relation and in the molecular backbone structure at a Peierls transition.

2.2 Conduction mechanisms

The polymers used are poly(p-phenylene vinylene)s (PPV). This is a so called π-*conjugated* polymer. 'Conjugated' indicates a string of alternating single (σ-bond) and double (a σ- and a $\pi-$ bond) bonds in the structure formula, which is important for the conductivity. The chemical structure of PPV is, among some other important conjugated polymers, given in figure 2.2. Trans-poly-acetylene, which consists of carbon atoms alternating bound together with double and single bonds, is the simplest case, but the more complex PPV behaves in many respect very much in the same way.

2.2.1 Polarons, bipolarons and solitons, exciton

The semiconductor band model of conjugated polymers originates from a study of collective excitations of the polymer chains. In a molecular view one can distinguish several sorts of excitation, which all correspond with certain electronic states in a band model.

Two double or two single bond next to each other on the conjugated string is called a soliton [1]. A soliton is charged (0,+ or - depending on the electron occupation) and can conduct (move). A soliton can only exist in a symmetric one dimensional 'conductor' such as trans-poly-acetylene, which is explained by a symmetry argument (lattice energy on both sides of a soliton should be equal). It can be seen as a local suppression of the Peierls transition and the energy of a soliton is therefore mid-gap.

[1] Called like this because its mathematical description resembles solitary waves in field-theory

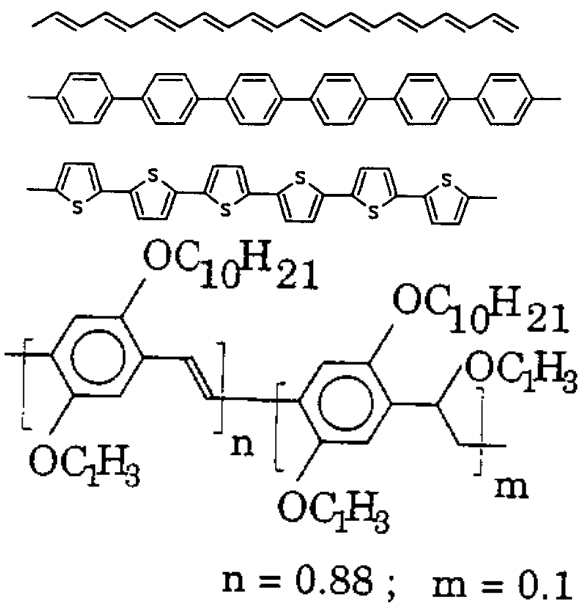

Figure 2.2: Chemical structure of several conjugated polymers. From top to bottom: poly-acetylene, poly-phenylene, poly-thiophene and OC_1C_{10}- poly(p-phenylene vinylene) (PPV).

Two solitons (a positive and a negative one) next to each other are called a *polaron*. A polaron is really a hole/electron pair, which has deformed the surrounding lattice. The two solitons of which it consist interact, are bound together, as a molecule, and the corresponding energy states are therefore no longer mid-gap but moved to the valence band and conduction band (The energies of the associated hole and electron are lowered). Polarons can also exist in other polymers than poly-acetylene, like PPV and poly-thiophene.

Bipolarons are pairs of polarons. A polaron is captured in the potential minimum of the other.

Polarons and solitons are in the band model principally localized states, in the band gap. In the molecule exciton model on the other hand, localization of electrons is inducted by the deformation amongst the chain molecules

It is unclear which mechanisms, or which kind of electronic states precisely are responsible for the conduction of the polymers. In the present study we use a simple view of a conduction and a valence band, with electrons and holes. They have however a small mobility, which is chosen field dependent, which reflects their principal localization or the possiblity of them continuously being trapped and untrapped in shallow localized states.

2.2.2 Hopping conductivity

In both semiconductor band model and the molecular model the charge carriers are in localized states and therefore the conduction of electrons in the conduction band and holes in the valence band is not an ordinary one, but is described by a *hopping* process

(phonon assisted tunneling). All states are more or less localized and to move (to conduct) a carrier must tunnel to one of its neighbor electronic states. Such a tunneling event has a probability which increase exponentially with the electrical field. Describing this effect with the microscopic mobility it will become field dependent [3, 57].

$$\mu(E) = \mu_0 \frac{\sinh(\alpha E)}{\alpha E} \tag{2.1}$$

Which is a sinh-function (sum of to exponentials) because a carrier can hop up- and downwards the field.

The field dependence is only important at high voltages.

2.3 Band-structure

As mentioned, a sample is often understood with a simple band-model as shown in figure 2.3. The possible energies of an electron are indicated as a function of its position. In

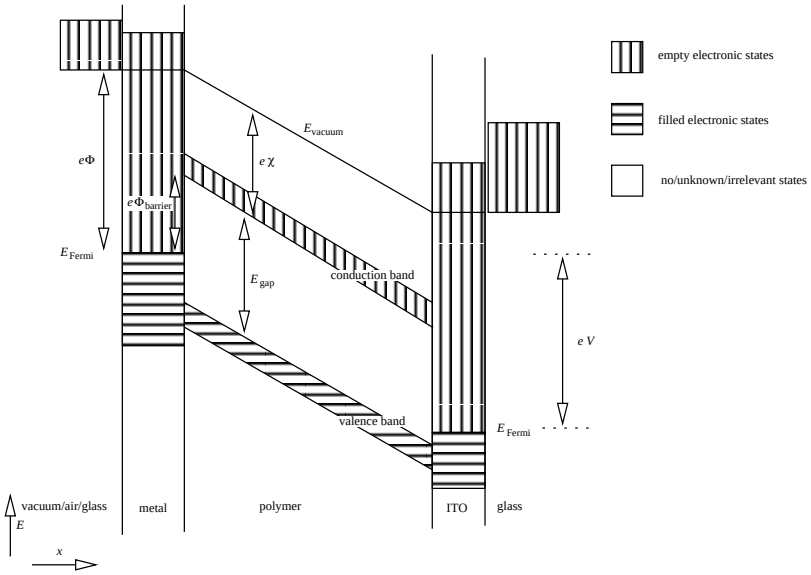

Figure 2.3: Simplified band-structure of a biased sample. Barrier lowering and band bending are not pictured.

this figure five areas are indicated of which the middle three form the actual sample under study. The outer two areas represent the nearby environment, which is on one side (the right side in figure 2.3) the glass substrate and on the other air or, in the case the sample is encapsulated, a glass plate which is glued against the sample.

Left from the polymer, in figure 2.3, is indicated the electron-injecting metal. Of course it is possible that this metal has energy gaps between the Fermi-level and the vacuum level, but this is of no importance in this study. Electrons on the Fermi-level need to gain an energy of $e\Phi$ to escape from the metal into the vacuum. This potential Φ is called the

work-function of the metal[2].

In the polymer two energy (potential) differences are indicated in figure 2.3. The *band-gap* E_{gap} is, as usually, the energy an electron must gain to excite from the valence to the conduction band. The potential χ is the *electron affinity* of the polymer, the potential difference between the bottom of the conduction-band and the vacuum level.

On the interface between the metal and the polymer arises a potential difference between the Fermi-level in the metal and the lowest unoccupied electronic states in the conduction band of the polymer. This potential-barrier Φ_{barrier} can, in this simple model, be calculated following:

$$\Phi_{\text{barrier}} = \Phi - \chi \tag{2.2}$$

In reality equation 2.2 is not always a good description. It appears that often this barrier is less strongly dependent from the work-function of the metal Φ then is expected from equation 2.2.

In semiconductors Silver and Shaw [53] claim 2.2 only to be true if the semiconductor has a high degree of ionic bonding. If the bonding is covalent Φ_{barrier} is independent of the metal work-function Φ. The reason covalently bond materials don't obey equation 2.2 is supposed to be due to localized electronic states on the interface, so called interface or surface states (see [66, 4, 46, 47]). These interface states 'pin' the Fermi-level of (any) metal relative to the energy-levels of the bulk material. It has been reported that this pinning occurs often around $\frac{2}{3}E_{\text{gap}}$ below the conduction band (see [47]).

For metal/polymer interfaces it is not clear whether the dependence of the barrier height Φ_{barrier} is following 2.2. Although Parker [55] claims it to be.

The original goal of this study was the determination of the barrier height , as it arises for electrons in the metal/polymer contact of interest (mainly Ca/PPV).

On the other side the polymer is bordered the transparent hole-injection ITO-contact. The barrier for holes from the ITO-contact to enter the polymer (in figure 2.3 the distance from the Fermi-level in the ITO and the top of the valence band of the polymer) cannot be measured directly using a photo injection experiment while the ITO is transparent [3]. Parker [55] found, using a tunnel injection model and MEH-PPV, a barrier of 0.2 eV for this barrier.

If both barrier heights are low enough to supply carriers to the polymer, both electrons and holes will contribute to the conduction of the sample. Because there is a chance an electron in the conduction band of the polymer recombines with a hole in its valence band, eventually emitting a photon, luminescence-efficiency is optimized if both carriers are available in equal amounts. Asuming equal mobilities for holes and electrons the same barrier height on both contacts would be best.

In figure 2.3 the Fermi-levels of the electron-injecting metal and the ITO are not equally high. This means that the sample is applied a voltage to, which is indicated as V.

[2] See for a list of work-functions e.g. [32, 56, 72]

[3] Although low-energy photons will partially absorb in the ITO-layer, the transparency of ITO is due to its plasma frequency, and not due to lack of electronic states, but this is no subject of this study. See [32] chapter 10 for a treatment of this phenomenon.

2.3.1 Build in Voltage

Due to the difference of work functions of the Ca and ITO contacts, a build-in voltage will exist at zero bias. If the sample is short-circuited, causing the Fermi-levels of the metal and the ITO to be equally high, an internal electrical field in the polymer occurs, because

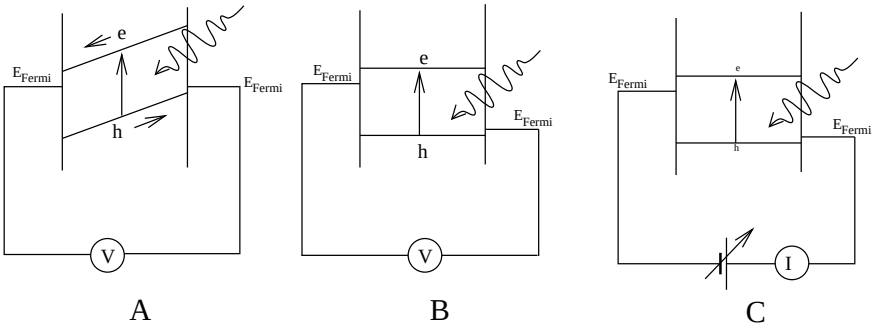

Figure 2.4: Illustration of the build-in voltage of a sample. Energy vs position plots are combined with electrical schemes.

the two barriers will remain unchanged. The voltage over the polymer is then called the *build-in voltage*.

As illustrated in figure 2.4A and B a photo-voltage will occur when illuminating the sample with above band-gap photons. Due to the build-in field electrons and holes will flow to opposite sides until the external voltage neutralizes the internal build in voltage. This is the situation in figure 2.4B. The build in voltage can be measured in this way (simply measuring the voltage over a illuminated sample), but a more accurate method is the one shown in figure 2.4C. The build in voltage is the voltage which must be applied to the sample to obtain minimal current.

2.3.2 Band bending

In all preceding pictures the bands were drawn with straight lines. This is not always an accurate view. Putting a semiconductor against a metal, will cause bands which are 'bend'. This can be seen as adjusting the Fermi level of the polymer to the Fermi level of the metal-contacts, (the barriers on the interface do not disappear) with the help of thermally injected carriers.

In an insulator only very few charges will inject, in case the sample is unbiased, only little space charge is build up, and the band-bending is very small. A realistic electrical field, implicating the potential, as function of place will be given on page 41.

2.3.3 Photo-conductive mechanisms

Illuminating the sample several photo transitions of electrons can occur (Reucroft in [57]).

- *Photo-carrier generation via low energy (singlet) states in the polymer.*

- *Photo-injection of carriers from the electrodes.* Electrons or holes in the metal contact are excited to a higher energy and can enter the polymer in its conduction respectively valence band.

- *Band-to-band photo-conduction.* Electrons from the valence band are excited to the conduction band, leaving behind a hole. Photon energy must exceed the bandgap, in contradiction to photo-injection, where a photon energy smaller than the bandgap is sufficient.

- *Optical detrapping of trapped charge.* If the bulk material contains traps (states in the gap[4]) these can be filled or unfilled with light. Unfilling filled traps will give temporary more carriers and therefore photo-current. In a steady state the quasi-Fermi level will be closer to the conducting band (conduction band for electrons and valence band for holes) giving an increase of the effective mobility of the carriers.

The different mechanism are indicated in figure 2.5. In the next section the photo-injection

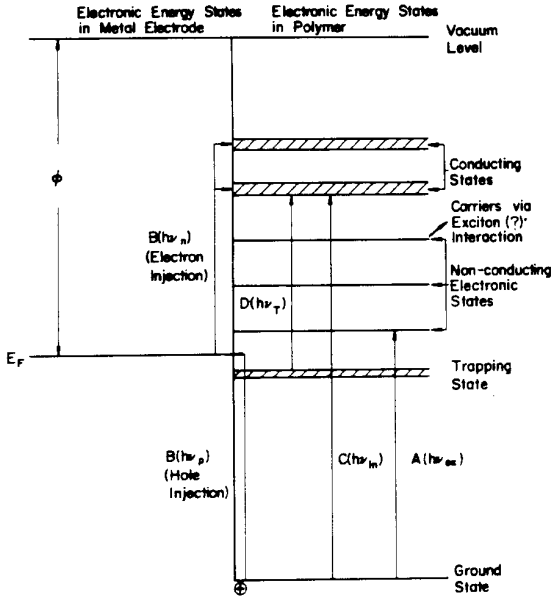

Figure 2.5: Processes leading to photo-excited carriers. The capital A–D correspond to the 4 in the text mentioned processes. Taken from [57].

mechanism will be studied further. This is the mechanism that is important in a barrier-height measurement. After that, attention will be given to the optical detrapping of charges. This can, while illuminating through the bulk, give rise to similar photo-currents as the photo-injection current, because the needed photon-energies are also well below the band gap.

[4] which can have many causes, such as the mentioned polaronic effects

2.4 Photo-injection

The process of injection electrons (or holes) from a metal into an insulator with the help of light is commonly known as internal photo emission (IPE) and as such it is often referred to in literature. In this work the term IPE has got the more general meaning of 'an increase of the current due to illumination, probably caused by improvement of the injection of electrons at the contact'.

The photo-injection theory is due to Fowler [21] and has been tested in a lot of experiments (e.g. [9, 29, 33, 35, 40, 43, 51, 52, 61, 77]).

The dependence on the photon energy of a photo-injection current is the same as for the so called external photo emission and will be described in the next paragraph.

2.4.1 External photo-emission, photon-energy dependence

Exciting an electron from a metal to vacuum is usually referred to as *external photo-emission*. The process of exciting an electron from the metal into an insulator's or semiconductor's conduction band (internal photo-emission) can be equivalently described.

The basic idea is that a photo-excited electron in the metal has a possibility of escaping the metal which depends on its direction. An assumption is that the photo excited electrons have a isotropic velocity distribution. The second assumption is that the electron escapes the metal when its velocity perpendicular to the interface is large enough to climb the energy barrier on the interface described in section 2.3.

Neglecting tunneling effects the photo excited electrons need an energy of at least $e\Phi_{\text{barrier}}$ above the Fermi-energy to escape from the metal.

Electrons can be excited from everywhere from the metal valence-band when illuminating with photons of energy E_{photon}, therefore electrons with energy between E_{Fermi} and $E_{\text{Fermi}} + E_{\text{photon}}$ will arise[5] (see figure 2.6). Of these, only electrons with an energy larger then $E_{\text{Fermi}} + E_{\text{barrier}}$ ($E_{\text{barrier}} \equiv e\Phi_{\text{barrier}}$) will have a chance to escape the metal. As mentioned, it will be assumed that an electron escapes only when it's momentum $p_\perp$ perpendicular to the interface will be large enough. The fraction of the excited electrons of a certain energy E satisfying this condition is proportional to the part S of the 'momentum sphere' in figure 2.7. The surface of S is (also called S)

$$S = \begin{cases} \int_0^\theta d\theta' 2\pi \sin\theta' p^2 = 2\pi(1-\cos\theta)p^2 & \text{if } p > p_{\min} \\ 0 & \text{otherwise} \end{cases} \tag{2.3}$$

,where the angle θ is defined in figure 2.7. And the fraction of all electrons with momentum p and $p_\perp > p_{\min}$ will be:

$$f'(p) = \frac{S}{4\pi p^2} = \begin{cases} \frac{1}{2}(1-\cos\theta) = \frac{1}{2}\left(1 - \frac{p_{\min}}{p}\right) & \text{if } p > p_{\min} \\ 0 & \text{otherwise} \end{cases} \tag{2.4}$$

[5] assumed is that the temperature is small, which is reasonable because the barrier-height is in the order of 0.1 eV and only $k_B T \approx 0.026$eV.

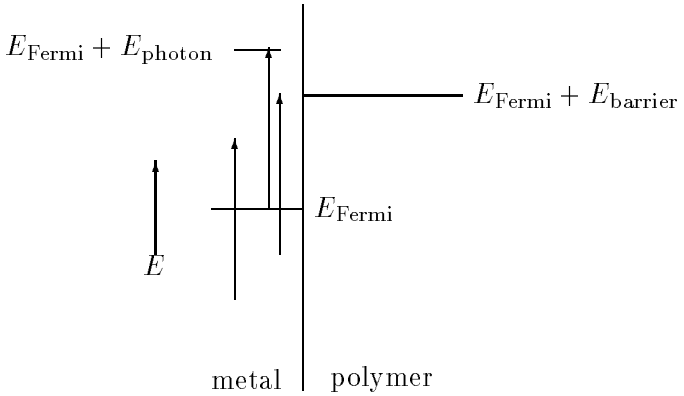

Figure 2.6: Electrons which can escape from valence band of a metal, when illuminating with E_{photon} photons (three arrows in metal). Left arrow: an excited electron which cannot escape to the polymer. Right arrow: an excited electron that can just escape to the polymer. Middle arrow: Excitation of an electron on the Fermi-level.

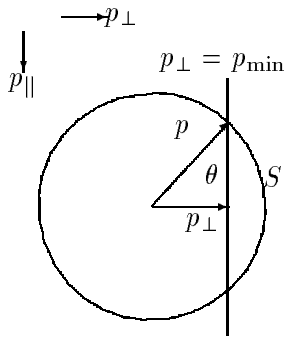

Figure 2.7: Momentum sphere (Drawn 2-dimensionally, the 3-dimensional equivalent is a trivially derived from this). The part of the momentum-sphere left of the plane $p_\perp = p_{\text{min}}$ is the part S that satisfies the escape condition.

As a function of electron energy this can be written:

$$f(E) = f'(\sqrt{2mE}) = \begin{cases} \frac{1}{2}\left(1 - \sqrt{\frac{E_{\min}}{E}}\right) & \text{if } E > E_{\min} \\ 0 & \text{otherwise} \end{cases} \tag{2.5}$$

where $E_{\min}$ is the minimum energy a electron needs to escape which is $E_{\text{Fermi}} + E_{\text{barrier}}$. The total fraction of electrons that will escape when illuminating with photons with energy E_{photon} is then (assuming $E_{\text{photon}} > E_{\text{barrier}}$)

$$\begin{aligned} Y(E_{\text{photon}}) &= \int_{E_{\text{Fermi}}}^{E_{\text{Fermi}}+E_{\text{photon}}} dE c f(E) = \int_{E_{\text{Fermi}}+E_{\text{barrier}}}^{E_{\text{Fermi}}+E_{\text{photon}}} dE c f(E) \\ &= c\frac{1}{2}(E_{\text{photon}} + E_{\text{barrier}} - 2\sqrt{E_{\text{barrier}}E_{\text{photon}}}) \end{aligned} \tag{2.6}$$

where $E_{\text{Fermi}} = 0$ is taken, and c stands for the density of states in the metal, assumed to be independent of the energy[6]. This formula can be 'Taylor-ed' around $E_{\text{photon}} = E_{\text{barrier}}$ to obtain:

$$\begin{aligned} Y(E_{\text{photon}}) &= \frac{c}{4E_{\text{barrier}}}(E_{\text{photon}} - E_{\text{barrier}})^2 + O\left((E_{\text{photon}} - E_{\text{barrier}})^3\right) \\ &\approx \frac{c}{4E_{\text{barrier}}}(E_{\text{photon}} - E_{\text{barrier}})^2 \end{aligned} \tag{2.7}$$

The quantity Y is called *quantum yield* and is the number of electrons injected to the polymer per absorbed photon. Assuming [7] that every injected electron will actually flow to the other side of the sample, Y is measured to be the current ('electrons per second') divided by the photon flux ('photons per second') on the sample.

2.4.2 Schottky barrier-lowering

Due to a image-force effect the barrier-height Φ_{barrier} is slightly dependent of the electrical field in the insulator near to the interface. Consider a metal-vacuum system first (The following is also very accurately explained in [72] chapter 5.3). When a charge, like an electron, is placed near to the surface of a metal it will feel an attractive force to it. This is because on the surface the electrostatic potential should be zero everywhere, which can be equivalently described by putting an equal, but opposite charge at the same distance on the other side of the metal interface. The attractive force, called the image force, is given by a simple Coulomb attraction between the charge and its image charge ($x = 0$ on the interface):

$$F_{\text{image}}(x) = \frac{-q^2}{4\pi\epsilon(2x)^2} = \frac{-q^2}{16\pi\epsilon x^2} \tag{2.8}$$

described by an image potential:

$$\phi_{\text{image}}(x) = \frac{-q}{16\pi\epsilon x} \tag{2.9}$$

[6] something will be said about this assumption on page 17

[7] It will appear that this assumption is not always valid.

If the sample is biased a charge also has an 'external' potential:

$$\phi_{\text{external}}(x) = -E_0 x + \Phi_{\text{barrier}} \tag{2.10}$$

where E_0 is the electrical field near $x = 0$. Both these potentials are plot in figure 2.8. The total potential:

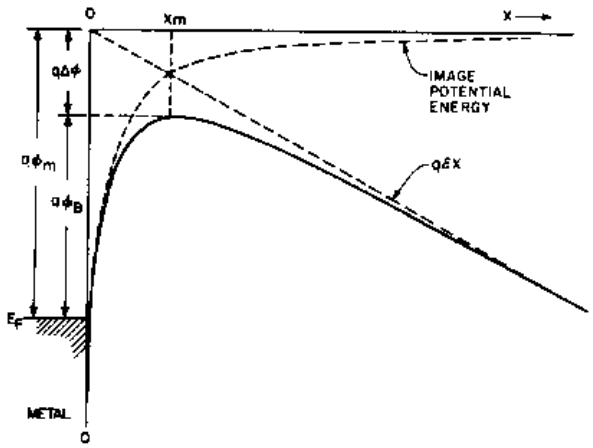

Figure 2.8: Image potential and External potential. (Taken from [72])

$$\phi(x) = \phi_{\text{external}}(x) + \phi_{\text{image}}(x) \tag{2.11}$$

has a maximum which can be found by differentiating it to x and putting it to zero [8]

$$\partial_x(\phi_{\text{image}}(x) + \phi_{\text{external}}(x))|_{x_m} = \frac{q}{16\pi\epsilon x_m^2} - E_0 = 0 \tag{2.12}$$

leading to an x_m (place of maximum):

$$x_m = \sqrt{\frac{q}{16\pi\epsilon E_0}} \tag{2.13}$$

Which leads to a barrier of:

$$\Phi_{\text{barrier}} - \sqrt{\frac{qE_0}{4\pi\epsilon}} \equiv \Phi_{\text{barrier}} - \Delta\Phi \tag{2.14}$$

where the *Schottky barrier lowering* $\Delta\Phi$ has been defined.

Measuring the barrier-height one should do this as a function of applied voltage. It should then be lowered following 2.14 (see [70]).

2.4.3 Dependence on electrical field

A photo excited electron which could enter the polymer will not always do so because there is a chance it will be scattered, in the metal, or before it reaches the actual barrier

[8] ∂_x is simply the operator which differentiates to x, often denoted by $\frac{\partial}{\partial x}$ or ∇_x. See for a list of symbols, uses in this report, appendix C.

on $x = x_m$ in the insulator. In such an event it can loose energy, so it may then have not enough to surmount the barrier, or its direction may become wrongly directed. The place and height of this barrier are, as was shown in the last paragraph, field dependent. The height will influence the minimal photon-energy at which photo-injection is possible. The place and shape of this maximum will influence the chance an hot electron will actually overcome the barrier.

The assumption is that the carriers thermalize at a distance x_0 from the injecting contact. Beyond this point the carriers are transported solely by the normal diffusion and drift processes. Between $x = 0$ and $x = x_0$ the problem is a more complex hot carrier problem. The number of carriers reaching x_0 is assumed to be proportional to the number of photo-excited carriers that could have surmounted the barrier in the simple model described in 2.4.1. The transport in the $x < x_0$ region is highly diffusive, so the applied voltage should have little effect.

Mort, Schmidlin and Lakatos [51] have derived an expression for the electrical field dependence of the quantum yield:

$$Y = \frac{\mu E}{\nu_R + \mu E} Y_0 \tag{2.15}$$

, where ν_R is the effective recombination velocity. For the derivation of this formula referred is to the original article [51].

It increases linearly with E at low fields and saturates (as $\mu E > \nu_R$) at high fields.

2.4.4 Narrow bands

In section 2.4.1 was found that the quantum yield varies approximately linearly with the photon-energy (equation 2.7). The assumption was made that both the metal valence band and the conduction band of the polymer were broad enough to carry the integration in 2.6 over the full range from $E_{\text{Fermi}} + E_{\text{barrier}}$ to $E_{\text{Fermi}} + E_{\text{photon}}$. If the conduction band of the polymer is smaller then $E_{\text{photon}} - E_{\text{barrier}}$ this is not justified. The density of states in the metal can of course also be different from a constant over the full range of energies. One can alter 2.6 easily to let it describe photo-injection from a small band into another small band. See figure 2.9 for explanation and definition of some used symbol. Two cases

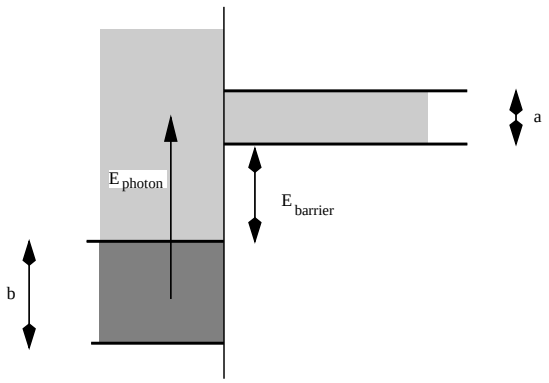

Figure 2.9: Photo-injection from a small band to another small band.

must be distinguished, $a < b$ and $b > a$. In the first case $a < b$ equation 2.6 is altered to:

$$Y = \begin{cases} 0 & \text{if } E_{\text{photon}} < E_{\text{barrier}} \\ \int_{E_{\text{barrier}}}^{E_{\text{photon}}} dEcf(E) & \text{if } E_{\text{barrier}} < E_{\text{photon}} < E_{\text{barrier}} + a \\ \int_{E_{\text{barrier}}}^{E_{\text{barrier}}+a} dEcf(E) & \text{if } E_{\text{barrier}} + a < E_{\text{photon}} < E_{\text{barrier}} + b \\ \int_{E_{\text{photon}}-b}^{E_{\text{barrier}}+a} dEcf(E) & \text{if } E_{\text{barrier}} + b < E_{\text{photon}} < E_{\text{barrier}} + b + a \\ 0 & \text{if } E_{\text{photon}} > E_{\text{barrier}} + b + a \end{cases} \tag{2.16}$$

and if $b < a$:

$$Y = \begin{cases} 0 & \text{if } E_{\text{photon}} < E_{\text{barrier}} \\ \int_{E_{\text{barrier}}}^{E_{\text{photon}}} dEcf(E) & \text{if } E_{\text{barrier}} < E_{\text{photon}} < E_{\text{barrier}} + b \\ \int_{E_{\text{photon}}-b}^{E_{\text{photon}}} dEcf(E) & \text{if } E_{\text{barrier}} + b < E_{\text{photon}} < E_{\text{barrier}} + a \\ \int_{E_{\text{photon}}-b}^{E_{\text{barrier}}+a} dEcf(E) & \text{if } E_{\text{barrier}} + a < E_{\text{photon}} < E_{\text{barrier}} + b + a \\ 0 & \text{if } E_{\text{photon}} > E_{\text{barrier}} + b + a \end{cases} \tag{2.17}$$

In these equations $f(E)$ simple represents:

$$f(E) = \frac{1}{2}\left(1 - \sqrt{\frac{E_{\text{barrier}}}{E}}\right) \tag{2.18}$$

and

$$\int_A^B dEf(E) = \left[\frac{1}{2}E - \sqrt{E_{\text{barrier}}}\sqrt{E}\right]_A^B \tag{2.19}$$

which can be filled in the above equations, to obtain for the quantum yield:

$$Y = c\cdot \begin{cases} 0 & \text{if } E_{\text{photon}} < E_{\text{barrier}} \\ \frac{E_{\text{photon}}+E_{\text{barrier}}}{2} - \sqrt{E_{\text{barrier}}E_{\text{photon}}} & \text{if } E_{\text{barrier}} < E_{\text{photon}} < E_{\text{barrier}} + \min(a,b) \\ E_{\text{barrier}} + \frac{a}{2} - \sqrt{E_{\text{barrier}}}\sqrt{E_{\text{barrier}}+a} & \text{if } E_{\text{barrier}} + a < E_{\text{photon}} < E_{\text{barrier}} + b \text{ and } a > b \\ \frac{b}{2} + \sqrt{E_{\text{barrier}}}(\sqrt{E_{\text{photon}}-b} - \sqrt{E_{\text{photon}}}) & \text{if } E_{\text{barrier}} + b < E_{\text{photon}} < E_{\text{barrier}} + a \text{ and } b < a \\ \frac{1}{2}(E_{\text{barrier}} - E_{\text{photon}} + a + b) + & \\ \sqrt{E_{\text{barrier}}}(\sqrt{E_{\text{photon}}-b} - \sqrt{E_{\text{barrier}}+a}) & \text{if } E_{\text{barrier}} + \max(a,b) < E_{\text{photon}} < E_{\text{barrier}} + b + a \\ 0 & \text{if } E_{\text{photon}} > E_{\text{barrier}} + b + a \end{cases} \tag{2.20}$$

2.4.5 Complete theoretical Fowler plot

Now we have reached the, in this work, most complete view of photo injection. For several voltages a barrier of 0.6 eV and bandwidths of 0.4 and 0.9 eV a theoretical plot was made in figure 2.10. The constant ν was chose large compared to μE. This model gives a reasonable realistic description of photon-injection into an insulator as shown for example by the measurements of Mort and Lakatos [35] of photo-injection of holes from gold into poly-N-vinylcarbazole (PVK) (and were reproduced by e.g. [29]). The picture of their result occurs very often in literature, it isn't absent here either. See figure 2.11. The decreasing of the quantum yield at higher photon energies is often obscured by the coming up of the band to band photo-conduction (at PPV at approximately 2 eV).

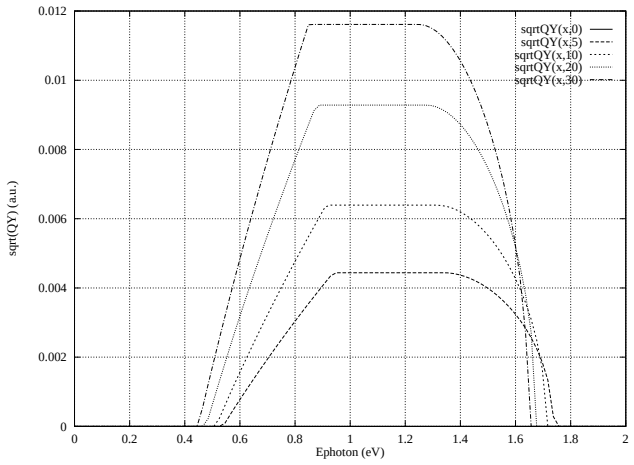

Figure 2.10: Theoretical Fowler plot for several voltages.

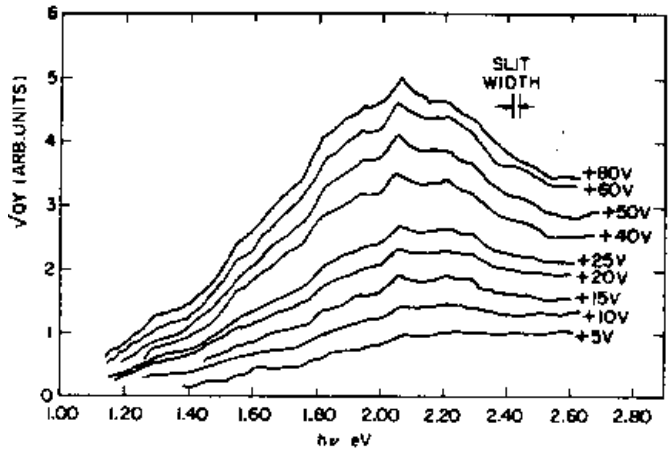

Figure 2.11: Fowler plot of photo-emission of holes from gold into PVK as measured by Lakatos and Mort (1968). Taken from [35].

At last I will remark that a quadratic dependence on the photon-energy of the quantum yield is not necessarily [50]. Other dependencies, such as $(E_{\text{photon}} - E_{\text{barrier}})^3$ or $(E_{\text{photon}} - E_{\text{barrier}})$ were suggested also. These can be modeled by taking account of the density of states function in equation 2.6, which was now taken to be constant (c) or a block-function (in 2.4.4). One can get any dependence on E_{photon} if one postulates this density of states function pathetic enough[9]. No further attention will be given to this.

2.4.6 Other injection processes

Of course a carrier can overcome the barrier on the interface in different ways also, otherwise it wouldn't conduct at all in the dark. Electrons (or holes) can tunnel through the barrier or they can thermally be excited over it.

Tunneling

A certain part of the current will be caused by electrons tunneling through the barrier. This tunneling chance through a triangular barrier (a Taylored WKB approximation, T=0, no image force) is given by (Fowler-Nordheim tunneling)

$$\kappa = \frac{8\pi\sqrt{2m^\star}(e\Phi)^{3/2}}{3eh} \tag{2.21}$$

and a current ([39, 55])

$$J_{\text{tunnel}} = \frac{e^2}{8\pi h\Phi} E^2 e^{-\kappa/E} \tag{2.22}$$

Parker [55] claims the carriers are injected in the polymer according to this mechanism.

Thermionic

It was assumed that above the Fermi-level no energy-level were occupied. Of course this is only acceptable relatively high above the Fermi-level or at sufficiently low temperatures. When $e\Phi_{\text{barrier}}$ is several tenths of electron-volts only very few electrons will have this energy thermally as follows from the Fermi-Dirac distribution-function:

$$f(E) = \frac{1}{\exp((E - E_{\text{Fermi}})/k_B T) + 1} \tag{2.23}$$

Room temperature ($k_B T \approx 0.026$ eV) and an energy of 0.2 eV above the Fermi-level lead to an occupation of 0.04%. The current is given by [72]:

$$J_{\text{thermionic}} = A^\star T^2 e^{-e\Phi/k_B T} \tag{2.24}$$

with the Richardson constant $A^\star$

$$A^\star = \frac{4\pi q m^\star k_B^2}{h^3} \tag{2.25}$$

[9] Density of states in metals are of course also measured. See e.g. [20, 56]. The valence band of gold has a width in the order of 10 eV, so taking the density constant in a range of 1 or 2 eV is probably not very bad.

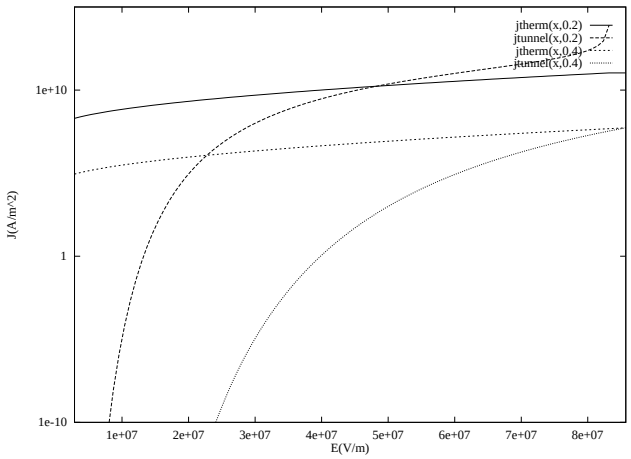

Figure 2.12: Tunnel and thermionic current through a triangular barrier of 0.2 eV (upper curves) and 0.4 eV (lower curves), not limited by diffusion, as a function of the electrical field on the contact. The thermionic current is only slightly dependent on the electrical field due to barrier lowering.

For low mobility semiconductors the injection current is not only limited by the contact, but also by the ability of the semiconductor to trespass the injected charge. Then the injection is diffusion limited, giving rise to [72]:

$$J = qN_C\mu E e^{-e\Phi/k_BT} \tag{2.26}$$

Also can the current be fully *space charge limited*, in which case the injection rate is totally irrelevant (as long as it is big enough to supply enough carriers for space charge limiting). This will be described in a next section.

Tunneling or Thermionic current?

To estimate what is a more important process when injecting carriers the currents of equation 2.22 en 2.24 are plotted in figure 2.12. As can be seen, Fowler-Nordheim tunneling is only an important process at very high fields. The maximum voltages which was applied to samples, in the experiments, was about 40 V at a sample of 700 nm thickness, which leads to a field of $5.7 \cdot 10^7$ V/m. On a contact of a space charge limited sample the field will normally be smaller. In the next section, where the IV-curves of a sample will be regarded Fowler-Nordheim tunneling injection therefore will be ignored.

2.5 Electrical description, sub-band-gap photo-conductivity

In the previous sections it was shown that the current through the sample could be increased by illuminating the contact. Carriers can more easily enter the polymer then. What happens when the polymer itself is illuminated (see also section 2.3.3)? In an experiment this is almost unavoidable.

If the polymer is illuminated with energetic photons, hole/electron pairs will be formed and the conduction will increase drastically. This, in the section about the build-in voltage already mentioned, phenomenon is called photo-conduction. The photon-energy at which the photo-conduction comes up is a estimation of the band-gap.

In the photo-injection experiments the energy of the photons will be well below the band gap, so no photo-conduction is to be expected. If the polymers contains however *traps* this may be different. A trap is nothing more then an electronic state in the gap. These states are (much more as 'conducting' states) localized, so no conduction through these gap-states is possible. Traps can be caused by pollutions or defects in the polymer, it can be the polarons of section 2.2.1,

Possibly, these traps can be filled or emptied with light. An empty trap can be filled with a photo-excited electron from the valence-band (in other words: a hole is photo-excited to the valence band) contributing to the conduction. A filled trap can be emptied causing extra electrons in the conduction band, again increasing the conductivity.

Before this effect can be studied more accurately, first we will discuss the IV-characteristic of a unilluminated sample.

2.5.1 Ohmic behavior

If the contact-barriers are low and the applied voltage very small, only few carriers will enter the polymer and one can assume that no space charge builds up (every injected carrier can flow to the other side unhindered by other carriers) ($\partial_x E = 0$) The current is simply given by:

$$j = (n + p)e\mu E = (n + p)e\mu V/d \tag{2.27}$$

or by the formulas which describe the current on the contact, given in section 2.4.6. This current is said to be *ohmic*. This behavior will occur in the samples under study at low voltages ($\approx$ 1V). The mobility can simply be chosen to be field dependent in this case.

2.5.2 Contact limited current

If the barriers are not low, and no space charge limiting occurs (at low voltages), the current is ohmic, but the barrier-height is influenced by barrier-lowering. So the j-V relation will not satisfy 2.27 but a term, caused by the barrier-lowering will enter.

2.5.3 Space charge limited currents

To calculate the space charge limited current two equations are of importance. Gauss' law[10]

$$\nabla \cdot E = \frac{\rho}{\epsilon} = \frac{e(p - n)}{\epsilon} \tag{2.29}$$

[10] In literature often referred to as the Poisson equation. Following Jackson [30] this however is

$$\nabla^2 \Phi = -\rho \tag{2.28}$$

,which is of course, with $E = -\nabla\Phi$, very closely related to Gauss' law.

and Ohm's law:

$$j = e(n+p)\mu E \tag{2.30}$$

where diffusion is neglected (it will be discussed on page 22).

From symmetry in the samples studied, argued is then that 2.29 can be written one dimensionally

$$\partial_x E = \frac{\rho}{\epsilon} = \frac{e(p-n)}{\epsilon} \tag{2.31}$$

Here E means the electrical field in the x direction, perpendicular to the layers in a sample.

One always find the applied voltage with:

$$\int_0^d dx\, E(x) = V \tag{2.32}$$

Single carrier, no traps

In the case just one carrier is involved, which cannot be trapped and the mobility μ is constant, the equations 2.31 and 2.30 are easily solved. They reduce to:

$$\begin{cases} \partial_x E = \frac{e}{\epsilon} p \\ j = p\mu E e \end{cases} \tag{2.33}$$

which leads to the differential equation:

$$\partial_x E = \frac{j}{\mu\epsilon}\frac{1}{E} \tag{2.34}$$

Integrating:

$$\begin{aligned} \int_{E_0}^{E(x)} dE\, E &= \int_0^x dx \frac{j}{\mu\epsilon} \\ \Longrightarrow E(x) &= \pm\sqrt{2\frac{j}{\mu\epsilon}x + E_0^2} \end{aligned} \tag{2.35}$$

E_0 is the electrical field on $x = 0$. This is fixed by the height of the barrier Φ and the current j. Integrating $E(x)$ leads to the voltage applied to the sample:

$$V(j) = \int_0^d dx\, E(x) = 2\frac{\mu\epsilon}{j}\frac{2}{3}\left(\left(2\frac{j}{\mu\epsilon}d + E_0^2\right)^{\frac{3}{2}} - E_0^3\right) \tag{2.36}$$

For a low barrier, E_0 is very small. Taking it zero we obtain the simple:

$$j(V) = \frac{9}{8}\mu\epsilon\frac{V^2}{d^3} \tag{2.37}$$

From equation 2.35 and 2.30 $p(x)$ is found:

$$p(x) = \frac{j}{\sqrt{\frac{2j\mu e^2}{\epsilon}x + E_0^2 e^2\mu^2}} \tag{2.38}$$

Which is maximal at the contact ($x = 0$). E_0 now can be estimated by making the assumption that the states in the valence band (we have dealt with holes in stead of electrons) are in thermal equilibrium with the states in the metal (Fermi Dirac):

$$p(x=0) = \frac{N_v}{e^{\frac{(\Phi - \Delta\Phi(E_0))e}{k_B T}} + 1} \tag{2.39}$$

with $j = p(0)e\mu E_0$ (or equivalently 2.38) this leads to an equation for E_0:

$$\frac{j}{E_0 e\mu} = \frac{N_v}{e^{\frac{(\Phi - \Delta\Phi(E_0))e}{k_B T}} + 1} \tag{2.40}$$

E_0 cannot be expressed in elementary functions of the quantities involved.

Single carrier, no traps, field dependent mobility

If the mobility is field dependent (equation 2.1) the single carrier problem can still be analytically solved. Equation 2.31 and 2.30 give together with the field dependent mobility 2.1 after integrating to $x = x$:

$$\begin{array}{l} \frac{\alpha j}{\epsilon\mu_0}\int_0^x dx = \int_{E_0}^{E(x)} dE \sinh(\alpha E) \\ \Longrightarrow \frac{\alpha j x}{\epsilon\mu_0} = \frac{1}{\alpha}\left(\cosh(\alpha E(x)) - \cosh(\alpha E_0)\right) \end{array} \tag{2.41}$$

We chose again $E_0 = 0$ to find:

$$E(x) = \frac{1}{\alpha}\text{arccosh}\left(\frac{\alpha^2 x j}{\epsilon\mu_0} + 1\right) \tag{2.42}$$

,which can be integrated from 0 to the thickness of the sample d to find the voltage as a function of the current j.

$$V(j) = \frac{\epsilon\mu_0}{\alpha^3 j}\left(\left(\frac{\alpha^2 j d}{\epsilon\mu_0} + 1\right)\text{arccosh}\left(\frac{\alpha^2 j d}{\epsilon\mu_0} + 1\right) - \sqrt{\frac{\alpha^2 j d}{\epsilon\mu_0}\left(2 + \frac{\alpha^2 j d}{\epsilon\mu_0}\right)}\right) \tag{2.43}$$

Unfortunately this cannot be written $j(V)$ in elementary functions.

The complete derivation can be checked by taking the limit $\alpha \to 0$, then the results of the previous paragraph are reproduced ($\lim_{\alpha\to 0}$ eq. (2.43) = eq. (2.37)) [11]

Two carriers, traps, field dependent mobility

If two kinds of carriers (electrons from one side, holes from the other) are injected in the sample the problem is not analiticly solvable[12]. So it was done iterative with a computer program, in which also traps and a field dependent mobility was taken account of. This program is described in chapter 3 and appendix A.

[11] Using e.g. the Mathematica-computer program, one can do this job quite quickly.
[12] But this fact in itself was not mathematically proved.

Diffusion

Diffusion of carriers is quite difficult to take in the calculations (the only way I could think of is a time solved simulation of the sample [13], which is very cumbersome). To illustrate it we look at the simplest case: one carrier, field-independent mobility, no traps, but diffusion:

$$\begin{cases} \frac{\epsilon}{e}\partial_x E = p \\ j = e\mu pE + eD\partial_x p \end{cases} \tag{2.44}$$

With the conditions:

$$\begin{cases} \int_0^d dx E(x) = V \\ E(0) = \text{given by barrier-height, e.g. } 0 \end{cases} \tag{2.45}$$

The diffusion coefficient D is given by the Einstein relation:

$$D = \frac{\mu k_B T}{e} \tag{2.46}$$

Which leads to the following inhomogeneous non linear differential equation of second order with boundary conditions:

$$\begin{cases} j = \frac{\epsilon}{e}\left(e\mu E\partial_x E + eD\partial_x^2 E\right) \\ \int_0^d dx E(x) = V \\ E(0) = 0 \end{cases} \tag{2.47}$$

Which has no known analytic solutions.

The importance of diffusion can however be guessed. In this simplest case (one carrier, no traps) the derivative of the carrier density is given by (from 2.38):

$$\partial_x p(x) = -\frac{j^2\mu e^2}{\epsilon}\left(\frac{2j\mu e^2}{\epsilon}x + E_0^2 e^2\mu^2\right)^{-\frac{3}{2}} \tag{2.48}$$

From equation 2.40 a value for E_0 was obtained for a barrier of 0.1 eV on a 10V, 700nm sample, and with equation 2.48 the diffusion current on every place in the sample was calculated and plotted in figure 2.13. This will give an idea of the error that was made neglecting diffusion currents.

As one sees the diffusion current could be important, for this particular voltage and barrier, only in the small area near the contact. For larger voltages and larger barriers this area becomes smaller. In the rest of the sample neglecting the diffusion current is justified.

2.5.4 Illumination

All arguments in this section will be applied to electrons and electrons traps. This is because it's easier, but the validity extends to holes and traps for holes naturally.

[13] So no longer solve equations iteratively, but a real simulation. Start with a sample biased at the build-in voltage and look what happens if suddenly a voltage is applied. In the first iteration no space charge is builded up, and one knows the electrical field and carrier-densities everywhere. This is not an equilibrium and you can iterate to the state of the sample on $t = dt$. Repeat this until nothing changes.

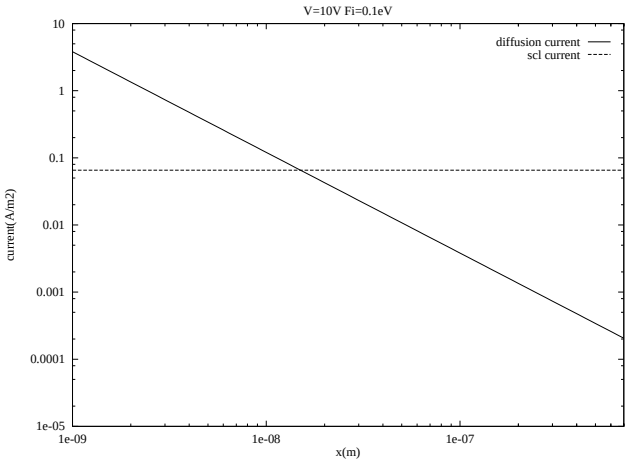

Figure 2.13: Estimation of the error made by neglecting the diffusion current, on every place in a 700 nm thick hole only sample. The current was calculated with a barrier and barrier-lowering. The diffusion-current is here described by a remarkably straight line, but very close to the contact it saturates.

When illuminating the polymer the simple thermal relation (which will be given as formula 2.51) between[14] $n \equiv n_f$ and n_t will change. Less carriers will be trapped. Because we are dealing with just two levels this can be modeled by using an other (higher) temperature. In the following the influence of the light will be calculated more directly.

Steady state

The assumption is that without illuminating a thermal equilibrium exist between the number of trapped carriers n_t and the number of free carriers n_f. This can be described as a dynamical equilibrium of a constant exchange of carriers in the traps (n_t) with carriers in the conduction band (n_f).

We define the rate s_{tf} (s_{ft}) to be the chance a trapped (free) electron will go to the conduction band (will be trapped) per unit of time. Steady state gives

$$n_t s_{tf} = n_f s_{ft} \tag{2.49}$$

We assume the trap chance s_{ft} to be proportional to the number of empty traps

$$s_{ft} = c_f(N_t - n_t) \equiv \frac{1}{\tau_f}(N_t - n_t) \tag{2.50}$$

Here τ_f could be seen as a 'life time' of a free carrier. This model must be consistent with the thermal result (Fermi-Dirac and Maxwell distribution):

$$n_t = \frac{N_t}{1 + N/n_f} \text{ with } N = N_c e^{-E_t/k_B T} \tag{2.51}$$

[14] n will be called n_f in this section for symmetry reasons

From 2.50 and 2.49 also an equation for $n_t(n_f)$ can be found

$$n_t = \frac{N_t}{1 + \frac{s_{tf}}{n_f c_f}} \tag{2.52}$$

so, to make these formulas equivalent:

$$s_{tf} = c_f N \equiv c_f N_C e^{-E_t/k_B T} \tag{2.53}$$

which is reasonable.

When illuminating the sample the traps can also be emptied by absorbing a photon so the rate s_{tf} will be bigger and called s^*_{tf}

$$s^*_{tf} = s_{tf} + s_L \equiv c_f N + c_L(N_C - n_f) \equiv \frac{N}{\tau_f} + \frac{1}{\tau_L}(N_C - n_f) \tag{2.54}$$

Here s_L has been postulated in the same way as s_{ft} was.

A new relation between n_t and n_f can be derived from 2.49 which now reads:

$$n_t s^*_{tf} = n_f s_{ft} \tag{2.55}$$

leading to

$$n_t = \frac{N_t}{1 + \frac{N + (N_C - n_f)\frac{c_L}{c_f}}{n_f}} \equiv \frac{N_t}{1 - c + \frac{N + cN_C}{n_f}} \tag{2.56}$$

, where c was defined. This formula can be approximated assuming $N_C \gg n_f$:

$$n_t \approx \frac{N_t}{1 + \frac{N + N_C c}{n_f}} \equiv \frac{N_t}{1 + \frac{N'}{n_f}} \text{ with } N' = N_C(e^{-E_t/k_B T} + c) \tag{2.57}$$

Using this equation in stead of 2.51 in calculations should give the current under illumination.

2.5.5 An alternative sub-band gap photo-conductive mechanism

A 'band' of mid-gap states could also lead to photo-conductive effects. Carrier in traps do have, in this case a small effective mobility. This band is however assumed to be a very 'bad' one, so it wouldn't effect the IV-curves of a sample noticeably. Only a very small current will flow through this band in comparison to the hole-current in the valence band or the electron current in the conduction band.

All numeric calculations were carried out without mobility in gap-states, but it is a possible improvement.

2.6 Bulk vs Supply limited currents

We have seen different mechanisms which contribute to the current-voltage behavior of a sample. These can be divided in two categories (as reflected in this chapter's setup).

Mechanisms on the metal/polymer interface(s) and mechanisms in the bulk of the polymer. Both these mechanisms can be influenced by illumination.

Photo-injection is a typical interface effect and the derivation of its describing formulas assumed that a photo injected carrier will flow unhindered to the other side. If the sample is limited by the contact, the photo-injection should not build up space charge in the bulk, arising a different current-voltage relation, or otherwise influence the bulk-conduction. One should therefore use very short illumination times (see [51]) because then only very few extra carrier (few compared to CV) are injected and they will not influence the bulk properties. This could also be achieved by using low light intensities. A simple photo-injection (IPE) experiment could thus only be done at a fully contact (or supply) limited sample.

If the contact barriers or the mobility of the bulk (and it is!) are very low, injected carriers cannot drain away freely and space charge limiting of the current will occur, injecting of extra carriers will have no effect on the current, so at a fully space charge limited sample it is impossible to do a photo-injection experiment.

One could avoid space charge limiting by using very short illumination times and also very short voltage biasing times, or by using a very low voltage. Only a few carriers are injected then, and no space charge can build up.

Chapter 3

Numerical

3.1 The program

In this chapter will be told how it was tried to calculate the current through a sample. This was done by the programs given in appendix A. Here will be given a short indication of the used algorithm.

A first remark is that not the current as a function of voltage ($j(V)$) was calculated but reversely $V(j)$. With a numerical inversion procedure [1] possibly $j(V)$ could be found. This is certainly necessary when calculating the photo-current, while the sample must be calculated twice then, at the same voltage.

The calculation of $V(j)$ is essentially a numerical integration of the electrical field E through the sample (formula 2.32).

The electrical field is calculated through the whole sample using Gauss' law (2.31). On every place therefore ought the carrier densities n en p to be known. They follow from Ohm's law (2.30). The already in the formula appearing electrical field is taken to be the nearest (spacely) already known value of E.

To be able to do this integrating at least on one point the values of n, p and E should be known already. This is not possible, but at a contact (the hole injecting one was chosen) one can know two of them. The electrical field on a contact is given by a for two carrier generalized version of equation 2.40:

$$j = \frac{N_v}{e^{\frac{(\Phi - \Delta\Phi(E_0))e}{k_B T}} + 1} E_0 e \mu_p(E_0) + n(x=0) e \mu_e(E_0) E_0 \tag{3.1}$$

And the carrier which is injected (holes) is given by the Fermi-Dirac function (formula 2.23).

The third quantity that should be known is then $n(x = 0)$. For a one carrier problem $n(x = 0)$ is chosen to be 0, otherwise something is guessed. This guess will afterwards lead to an electron density at the electron injecting contact ($x = d$) which should correspond with the barrier height. If not, the calculation is redone with a new guess for $n(x = 0)$. This is in fact also a numerical inversion procedure.

[1] Numerical inverses were done with a bisection or Newton-Raphson algorithm. See [12] and section A.

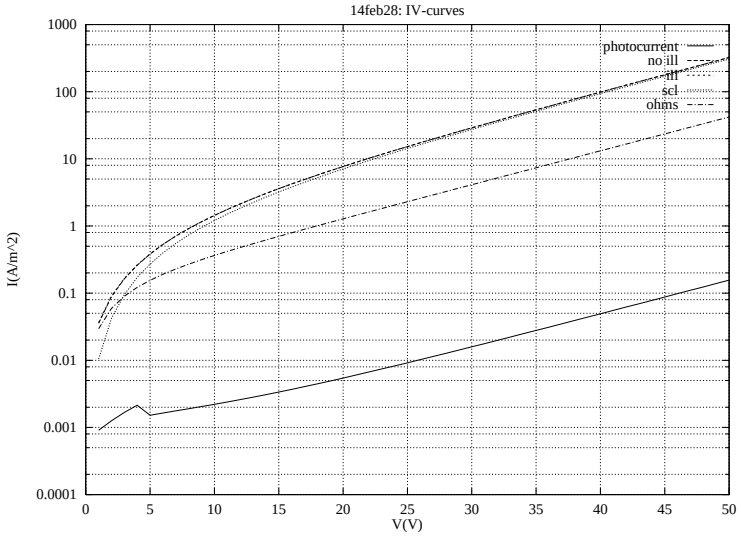

Figure 3.1: A calculation of a photo-IV curve. Used was a 2 carrier model with barriers of 1.8 (electrons) and 0.2 eV (holes) (very nearly single carrier). $1.5 \cdot 10^{23}$ hole-traps per cubic meter, 0.4 eV above the valence band. The Fermi level was chosen at 0.26 eV above the valence band, so the traps are full.

So the real heart of the program is a function which calculates $n(x = d)$ (really the associated barrier-height) and V at given $n(x = 0)$ and j. $n(x = 0)$ is varied until the electron barrier height equals the given electron barrier height. This whole procedure is repeated with different j until V satisfies the wanted voltage.

Everything can be done in presence of hole and electron traps. The occupation of them is given by the Fermi-Dirac distribution function (thermal equilibrium). Illumination changes this distribution (see section 2.5.4). The difference of two calculations, with and without illumination, leads to the searched photo-current. Also recombination of electrons and holes can easily be calculated, which can lead to the luminescence (where a Poly-LED of course was made for).

Above bandgap photo-conduction can also be calculated by introducing a negative term in the recombination. But this is no subject of this work.

3.2 Some results

Typical results of the program for the electrical field and carrier densities are given in chapter 5 on page 41. These results change very little under illumination.

3.2.1 I-V curves, photo-current

Some photo-currents, together with the associated IV-curves which were calculated are shown in figure 3.1 and 3.2

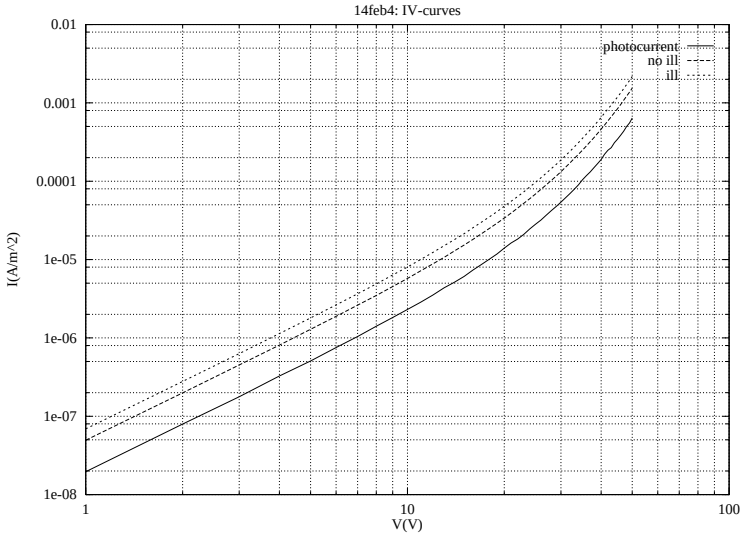

Figure 3.2: A calculation of a photo-IV curve. Used was a 1 carrier model with a barrier of 0.2 eV (holes). 10^{24} hole-traps per cubic meter, 0.4 eV above the valence band. The Fermi level was chosen at 1 eV above the valence band, so the traps are empty.

We see that both empty and full traps give rise to an additional photo-current, and that it is more or less proportional to the total current,

Chapter 4

Experimental

4.1 Structure of a sample

The used samples were 3x3 cm glass substrates on which Indium-Tin-Oxide (ITO)- contacts were evaporated. On this a layer of the polymer was spin-coated. A layer of another metal (Ca, Au, Al, In, etc.) was evaporated on the polymer then. This was done with a shadow mask, to structure it. The ITO was structured by means of etching. If the metal is very reactive, like calcium, the electrode is covered with a second metal layer in order to protect it. To screen the polymer from the air the sample is packed with another piece of glass and glue, except, of course, the endings of the ITO- and metal-contacts. In this way several ITO/polymer/metal devices were produced on one sample (usually 4). A schematic view of a sample is given in figure 4.1

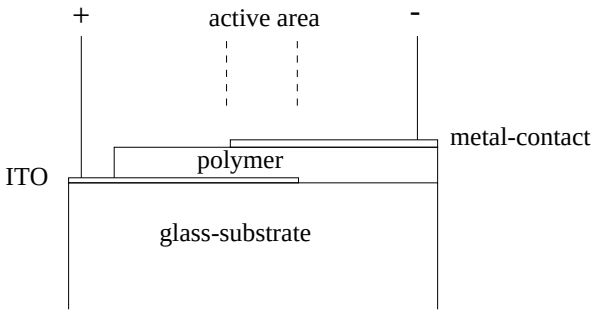

Figure 4.1: The structure of a sample

Spin-coating is a technique to make thin layers of a soluble polymer of a relatively homogeneous thickness. A drop of a solution of the polymer is dropped on a rotating substrate. Dependent of the viscosity of the solution and the rotation speed, a layer of a certain thickness is formed after the solvent is evaporated. No stretching or otherwise ordering steps are performed and the polymer chains are randomly, or at least in an unknown way, distributed in the layer.

4.2 Photo-current setup

To measure the photo-current a setup is used as schematically shown in figure 4.2. Essentially

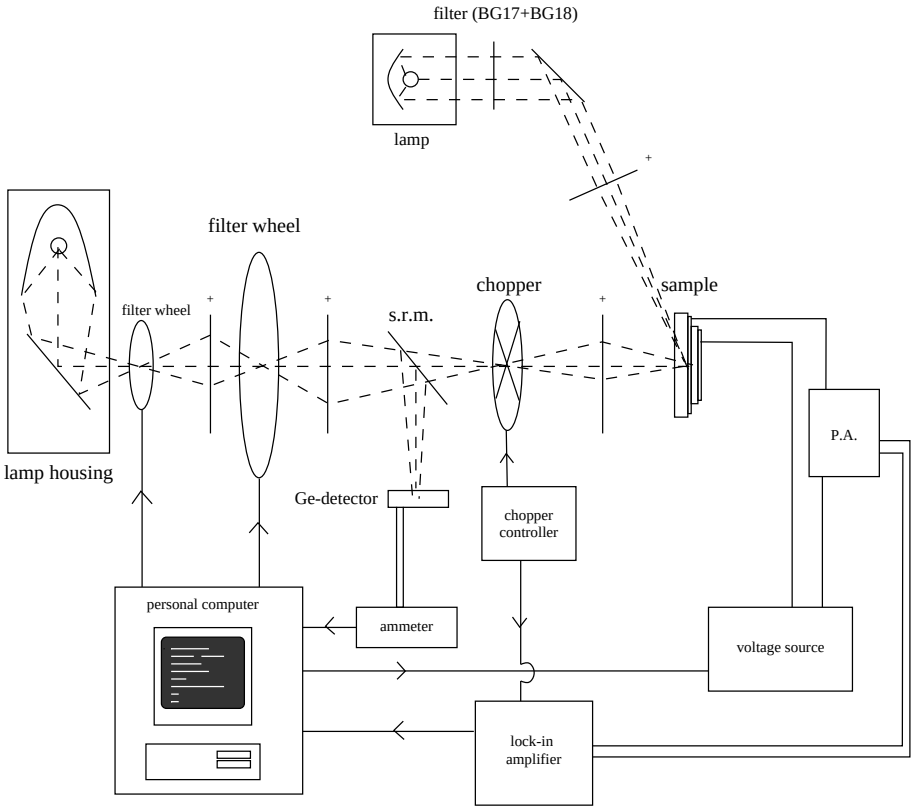

Figure 4.2: A schematic view of the used experimental setup. 's.r.m.' Stands for 'semi reflecting mirror' and P.A. for 'pre-amplifier'. Solid lines between object symbolize electrical wires or merely, with an arrow, flows of information. The dashed lines indicate some possible paths of the photons from the Xe (Hg)-lamp.

this setup measures the additional current caused by illuminating the biased sample with infra-red or visible light. This is not done by simply measuring the current through the sample because this additional current can be very small and undetectable in the large dark-current [1]. By chopping the light this additional current gets a well-defined frequency. With a lock-in amplifier [2] (LIA) this kind of frequency modulated signals can be filtered out very accurately. The LIA is referenced with a 1V square signal from the chopper driver with the same frequency as the chopped light. Naturally, the light from the Xenon-lamp

[1] However, often the signals were large enough, especially after a few seconds' illumination, to be measured with a ordinary ammeter.

[2] A lock-in amplifier is an electronic device which is widely used as a technique for getting small signals out of its noise. More generally it can be used to filter out the signal the part with a certain frequency. An example of the last is a measurement of photo-induced absorption. In these experiments the sample is illuminated with a laser to excite it and the absorption of light of another source (usually a much lower photon-energy) is measured. The probe light should be chopped and the transmission is measured with a lock-in referenced with the chop-frequency. See for a good theoretical description [18].

interference filter (nm)	energy of transmitted photons (eV)	blocking filter
1950 ± 5	0.636 ± 0.002	Ge-filter
1800 ± 5	0.689 ± 0.002	Si-filter
1570 ± 5	0.790 ± 0.003	,,
1300 ± 5	0.954 ± 0.004	,,
1200 ± 5	1.033 ± 0.004	RG8
1100 ± 5	1.127 ± 0.005	,,
1050 ± 5	1.181 ± 0.006	,,
1000 ± 5	1.240 ± 0.006	,,
950 ± 5	1.305 ± 0.007	,,
900 ± 5	1.378 ± 0.008	,,
848 ± 5	1.462 ± 0.009	,,
795 ± 5	1.560 ± 0.010	,,
750 ± 5	1.653 ± 0.011	,,
700 ± 5	1.771 ± 0.013	OG4 50.50.2
647 ± 5	1.916 ± 0.015	,,
598 ± 5	2.073 ± 0.017	,,
546 ± 5	2.271 ± 0.021	BG39 + KG3
491 ± 5	2.525 ± 0.026	,,
460 ± 5	2.695 ± 0.029	,,
430 ± 5	2.883 ± 0.034	,,

Table 4.1: The used filters in the both filter-wheels

should be monochromated, because the interest lies in the frequency of the light dependence. This was achieved with suitable interference filters. Twenty of them were available and were mounted on a wheel. The needed filter could be selected with the help of a stepping motor drive. Multiples of the wanted frequency were filtered out with an additional blocking filter. These blocking filters were, like the interference filters, also mounted in a filter wheel. In this wheel a non-transmitting site was constructed also so the illumination of the sample could be interrupted easily. The used interference filters have an approximate bandwidth of 5 nm. The filters, with associated blocking filter, used are given in table 4.1. The blocking filter are band or cut off filters.

A fraction of the monochromated light was split off with a semi-transparent mirror (a beam-splitter). The intensity of this reflected part of the light was measured with a germanium-photo-detector. To be able to extrapolate this to the intensity of the light on the sample itself, the arrangement was calibrated by using a detector on the place of the sample. A second detector was not readily available so the calibration was done with just one. Reproducible results were obtained by averaging the readout of the detector over a long time (several minutes) on both places. A small wavelength-dependence of the found ratio TRANS was found. TRANS had been defined as

$$\mathrm{TRANS}(\lambda) = \frac{\text{averaged readout of the detector on the sample-spot}(\lambda)}{\text{averaged readout of the detector on the reference spot}(\lambda)} \qquad (4.1)$$

This wavelength-dependence is due to wavelength dependent responses of the semi transparent mirror and the lenses in the setup. This calibration TRANS is given figure 4.3.

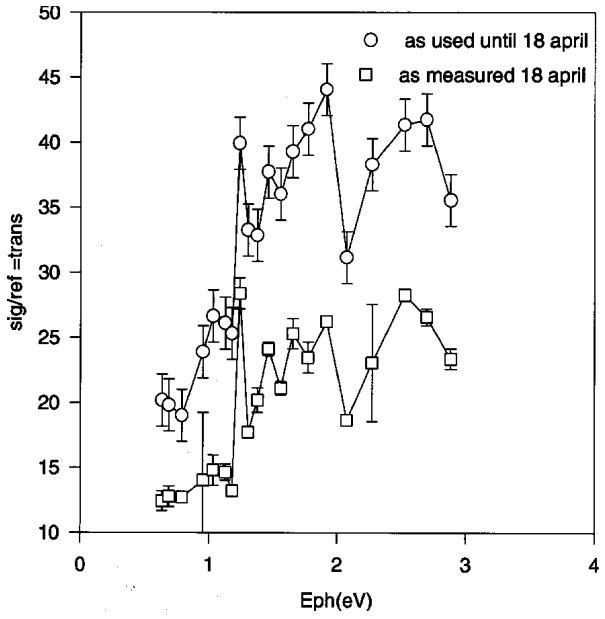

Figure 4.3: The calibration of the arrangement from the photo-detector up to the sample

With the calibration of the detector one can calculate the number (n) of photons falling per second on the sample following:

$$n(\lambda) = C\frac{i \cdot \mathrm{TRANS}(\lambda)}{c_{\mathrm{Ge-detector}}(\lambda) \cdot E_{\mathrm{photons}}(\lambda)} \tag{4.2}$$

with: i : current through detector (A)
$c_{\mathrm{Ge-detector}}$: calibration of the detector (A/W)
E_{photons} : Energy of the photons (J)

The constant C in this equation is in a first approximation the ratio of areas of the hole in the detector and of the sample. It is not impossible that this constant is slightly wavelength dependent, but the goal is to let it not be, and so it is assumed. Because the interest lies not in absolute values but in dependencies from photon-wavelength, the precise value of this constant is not very important. For simplicity $C = 1$ is chosen.

To the sample a bias voltage can be applied with a keithley 220 voltage source. The current through the sample is amplified with a current sensitive pre-amplifier (PA) which gives a voltage as output. This voltage is measured with a lock-in amplifier (LIA) referenced with the chop-frequency of the light. In this way just the current caused by the illumination is detected. Usually this current is only a very small fraction of the total current.

The LIA, the both filter-wheels, the voltage source and the reference germanium diode are all read out and/or set by a personal computer (PC). This PC is working with a Pascal program [48] written especially for this purpose (Turbo Pascal 6.0 Rikken, Kessener and Meeuwissen).

It should be remarked that the extra lamp in the setup of figure 4.2 could be used to do a dual beam photo conduction experiment. In such an experiment the sample is continuously

illuminated with 'bias'-light (see [75]). This element was only placed in the setup at the end of this research and it didn't yet lead to interesting results.

4.2.1 Chop-frequency of the light

The used devices can be quite well modeled using a mobility of the carriers in the polymer $\mu \approx 1 \cdot 10^{-10}$ m^2/Vs ([5]). It is field-dependent and will be higher with higher fields. The drift time τ for a carrier to cross an entire sample can be roughly estimated to be:

$$\tau = \frac{d^2}{V\mu} \tag{4.3}$$

A large thickness of 700 nm and a low voltage of 5 V leads to an estimation $\tau \approx 10^{-3}$ s. Using a chop-frequency of the light of 40 Hz the sample will be illuminated in $2.5 \cdot 10^{-2}$ s intervals, substantially longer then τ so steady state was supposed to be neared. This is of importance when comparing the measured results to the numerical calculation, which is based on this assumption. For a good photo-injection experiment it would be best to use short pulses, and to avoid space charge limiting, as was explained in section 2.6.

Under more favorable conditions a signal was measured as a function of this chop-frequency resulting in figure 4.4 As is to be seen in this figure the quantum yields depends heavily on

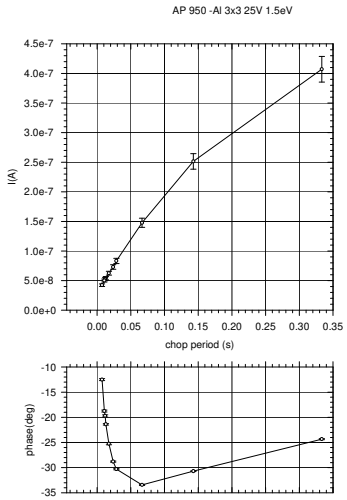

Figure 4.4: Measured QY as a function of the chop frequency. Uses was a sample of about 500 nm thickness polymer KTB26 and an Al-cathode, applied with a voltage of 25V.

the chop frequency. When longer illumination intervals are used the signal becomes larger, suggesting that steady state is not reached, not even after several tenths of a second.

Measuring of the current as a function of time, under continuously illumination suggest that the photo-current can increase for hours, but that it goes less fast after several tens of second. This is illustrated in figure 4.5 and in the next chapter (see page 47).

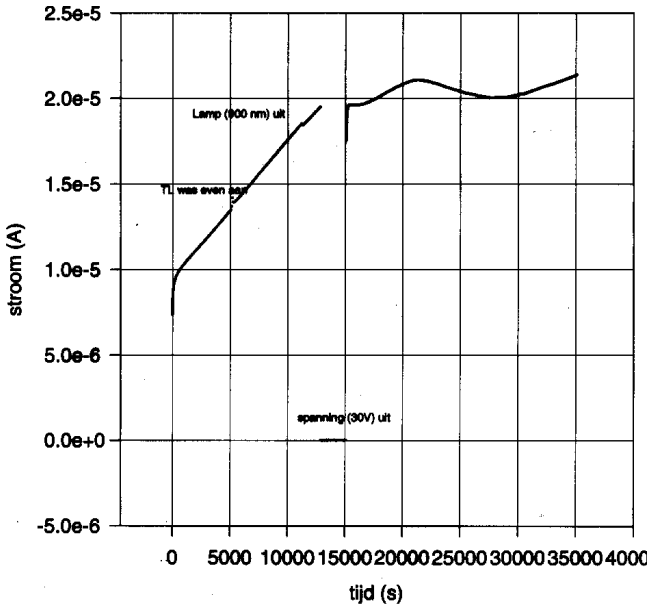

Figure 4.5: The current through a sample as a function of time. We see a fast increase in the first few seconds. Moreover we see in this measurement several other events, which influenced the current. We see a little peak at 5000 s which was caused by turning on the light in the set-up room. Further we see a little step at approximately. 12000 s where the illumination of the sample with 900 nm light was turned of. At approximately 13000 the biased (30 V) was turned of, and therefore no current can be seen anymore. When it's turned on again the signal becomes approximately as big as it was just before the turning of, but behaves unpredictable.

4.3 The construction and use of the measurement-program

All measurements were carried out by a computer programmed with a Turbo Pascal program [48]. This program was based on the original program by Rikken and Kessener, but it was virtually rewritten. The program now deals with all kinds of measurements, not only IPE-spectra. The error in a measurement is now estimated by taking the standard deviation in the repeated measurements (repeated it already was, but nothing more then taking the mean and throwing away some points was done).

The program has to wait on several points in the program for the lock-in. It would be cumbersome to describe here (for the reproducibility) the exact procedure the program follows. Therefore the important parts of the program that measure e.g. the photo-current are given in appendix B.

4.4 Difficulties

A difficulty is that the LIA will always give some signal, even when the signal is below the detection limit (signal<noise). Because of the normalization with the photon-density one will just see the inverse photon-density then. Above the detection limit (signal>nois2e) the signal certainly is proportional to the light-intensity, and should therefore be divided by it. If not, the photon-energy dependence of the undivided signal is largely photon-energy dependent as the source is. In principle the program deals partially with this problem, by subtracting a signal at zero intensity. To demonstrate this problem once can measure no sample, or not illuminate it. In this case there is certainly not a signal, because there's simply nothing to measure. Obtained is then for example the IPE-spectrum of figure 4.6. We see that even now a structure appears. Comparing it with the measured inverse light if figure 4.7 intensity we see directly the correlation.

4.4.1 Proportionality to light intensity

The measured signal can also obtain structure if the signal is not linearly proportional to the light intensity, but is related in some other way to each other (e.g. proportional to some power of light intensity). This can be simply tested by varying light intensity against the signal (QY). This was done and lead to figure 4.8. As can be seen the signal is relatively independent of light intensity (as expected) at higher intensities. Therefore the intensity must be chosen high enough, to assure that the photon-energy-dependency is due to the photon-energy and not due to the photon-energy-dependency of the intensity.

4.5 Mean free path of hot electrons

To avoid problems of absorbing photons in the bulk of sample one could think of illuminating the cathode not through the polymer, but from the other side. Hot electrons are then produced which should travel through the metal to the metal/polymer interface, where

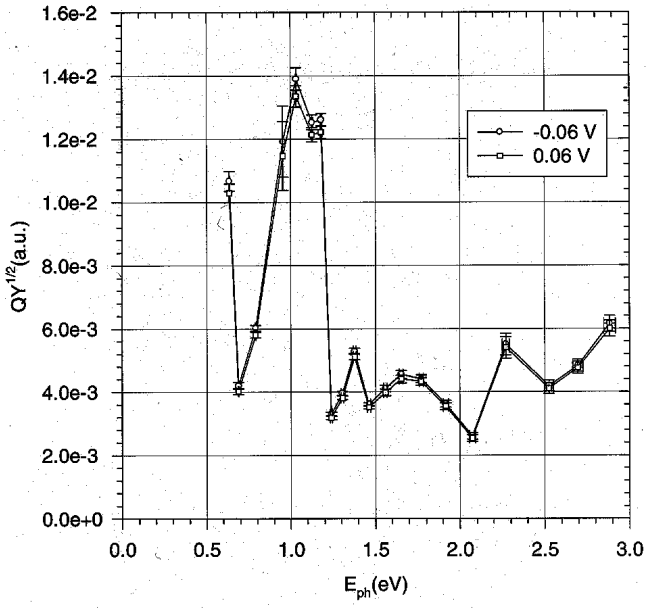

Figure 4.6: The IPE-spectrum of sample illuminated from the gold side of a Au/T_{12}/ITO-sample. The gold was obviously too thick and the signal is below the detection limit at every photon energy.

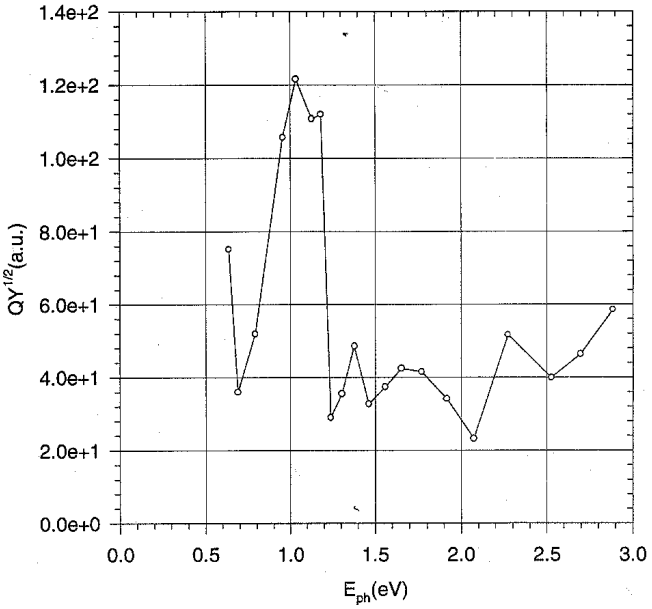

Figure 4.7: The inverse light-intensity of the lamp vs. photon-energy. While an IPE-signal is divided by the light-intensity, a undetectable small signal will be proportional to this curve. For the signal, normally from the LIA, a constant (1), was used.

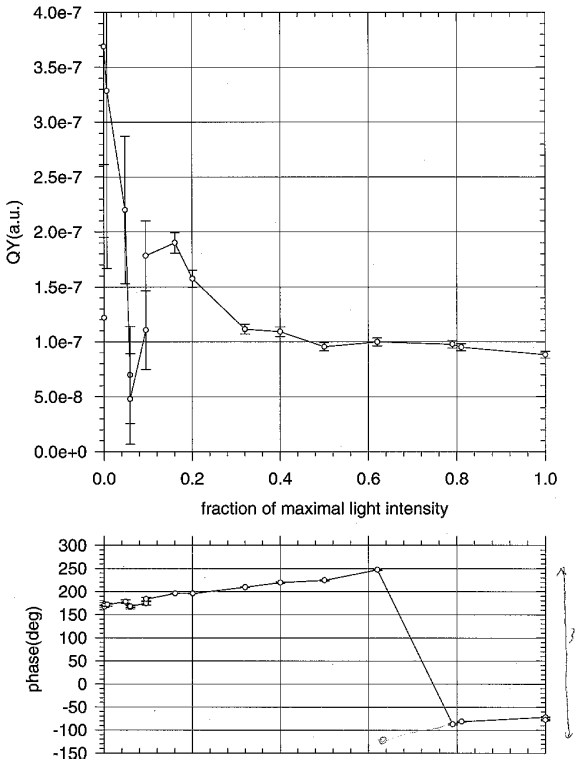

Figure 4.8: QY as a function of light intensity. A Hg lamp was used monochromated around 1.5 eV. An unconjugated Al/PPV-sample was used.

they could be injected described by Fowler theory[3]. The photo-excited electrons should not be scattered before reaching this contact or, in other words, the mean free path of these electrons should be substantially larger then the thickness of the metal layer. Preferably the metal-layer should also be thick enough to screen the polymer bulk from photons. Unfortunately the mean free path of hot electrons (or, of course, holes) in metals is quite poorly known [4] for most metals. For gold the mean free path of 1 eV electrons is about 70 nm (see [70, 19, 74, 31, 33]) and less for higher energies. A sample with a gold-contact of about this thickness should allow electrons (or holes) to enter the polymer when illuminating from the gold side. Unfortunately a gold-layer of this thickness will normally not screen all photons. Measurements of this kind did normally show the same as when illuminating from the ITO-side, or nothing at all as the layer was too thick.

[3]The escape cone will however be smaller, while electrons not moving perpendicular to the interface have to travel a longer way through the metal, thus having more chance to scatter.

[4]In fact a common technique of determining it are photo-injection experiments.

Chapter 5

Results and discussion

In this chapter the results of several done measurements are described and discussed for an explanation of them. Dealt is with the 'IPE' spectra of PPV and thiophene samples and several other kinds of measurements, time dependent and voltage dependent.

5.1 IPE-spectra of PPV-samples

'IPE' spectra were taken from ITO/PPV samples with Ca, Au, Al and In contacts, as a function of the applied voltage. Results are described in the following sections and a attempt to explain them will be made.

5.1.1 Au/PPV/ITO

An IV-curve of a Au/PPV/ITO-sample is given in figure 5.1. The slope of this log-log-IV-

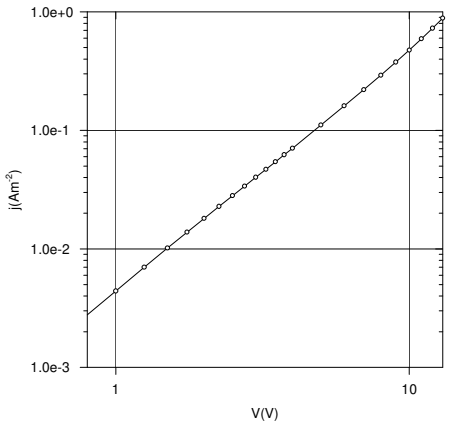

Figure 5.1: An IV-curve of a Au/PPV/ITO-sample [5]. Both scales are logarithmic.

curve is ≈ 2, which means that $j \propto V^2$ as in equation 2.37. Assuming a model without

traps and a single carrier (The ITO doesn't inject electrons), the assumption of a small E_0 (therefore a small barrier) is apparently correct. In other words: the current is fully space charge or bulk limited; the contact is not a limiting factor in the current at higher voltages.

A fit of the IV-curve to equation 2.37 lead to

$$\mu \approx 0.5 \cdot 10^{-10} \mathrm{m}^2/\mathrm{Vs} \tag{5.1}$$

where $\epsilon = 3.0$ was assumed (determined from capaticance measurements [63]).

The whole curve could be fitted to equation 2.36 with the help of a numerical program [5], which in principle leads to a barrier-height for holes entering the polymer. In practice however only an upper limit of a few tenths of an electron-volt can be established.

Assumed was that no hole-traps were present, but this is not necessary. Results change little if only *filled* or few hole traps are present in the initial, unbiased, state of a sample.

In a space charge limited sample the electrical field is not a constant, it varies with place. As an illustration the electrical field was plotted as a function of place in figure 5.2C. This figure was obtained with the program described in chapter 3. Filled traps for holes were taken into the calculations and even electrons with traps. $p(x)$ and $p_t(x)$ are plotted also in figure 5.2B. Figure 5.2A gives a theoretical , numerically solved, IV-curve, as were also shown in chapter 3.

Au-samples are hole-only devices. In the forward and backward only holes are flowing. In the forward injected by the ITO and in the backward by the Au-contact. The other contact cannot inject electrons because the barrier for these is to high (nearly 2 eV). It can inject holes, but these will flow back, not crossing the sample, because of the electrical field.

Photo-injection?

In the IPE-spectra (figure 5.3) of Au/PPV/ITO samples we see remarkable 'beautiful' curves, even comparable to the measurements of figure 2.11 and the calculations of figure 2.10. The signal comes up at approximately 1 eV. From IV-measurements, and from the high gold-work-function, we expect that gold, on a PPV contact, will have a low hole and a high electron barrier. In the IPE spectra however we see little difference between the forward and backward curves. Assuming the signal is caused by photo-injection the barrier-height for holes and electrons should then be about equally high, contradicting the IV-curves.

A sample with a calcium in stead of a gold cathode gives in the forward a comparable IPE spectrum (see figure 5.4). The IV-curve(see 5.5) of a Ca-sample is asymmetric, in the reverse only a small current is present. Concluded was that Ca cannot inject holes into the metal, so the barrier for holes entering the polymer must be big (and because it does inject electrons it must be bigger than at least 1 eV). A calcium contact is therefore not like a gold-contact and a forward (injecting electrons) spectrum like that of a gold-sample contradicts a photo-injection explanation.

Concluded is that the observed photo-current signal is not due to photo-injection (internal photo emission) but due to an increase of conductivity of the bulk while illuminating it.

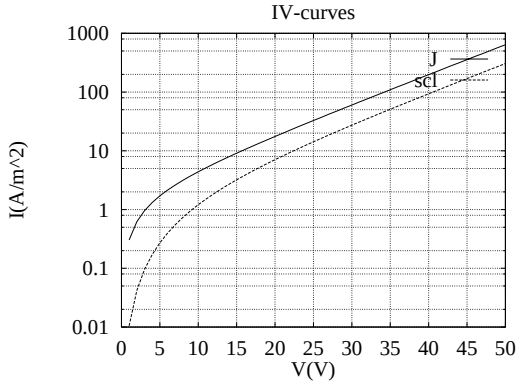

A. IV curve

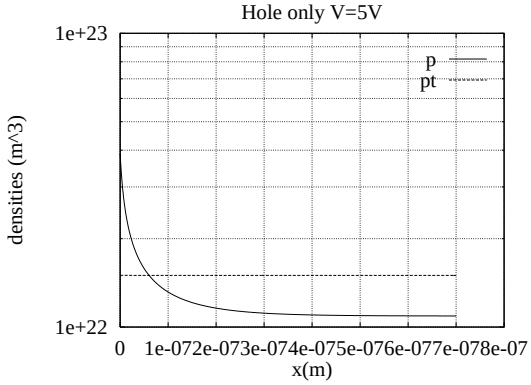

B. Hole densities (trapped and free)

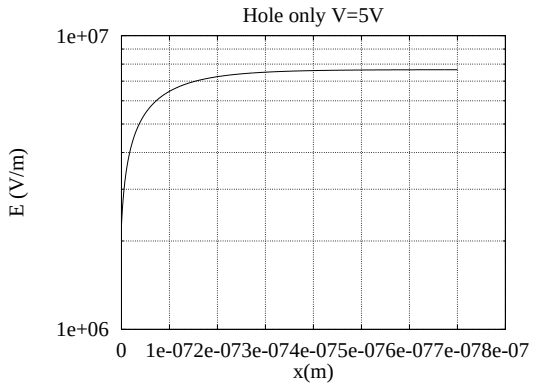

C. Electrical field

Figure 5.2: IV-curve, Electrical field and hole density in a hole-only sample. The calculations were carried out with the Fermi-level 0.2 eV above the valence band, Traps for holes 0.4 eV above the valence band (therefore full traps) and anode (hole injecting at x=0) with a barrier of 0.2 eV and a cathode (electron injecting at x=700 nm) with a barrier of 1.8 eV. A hole trap density of $1.5 \cdot 10^{22}$ /m^3 was used. Field dependent mobility was used also, but the effect is very small. Only very few electrons exist (maximal $1.5 \cdot 10^{-4}$ /m^3).

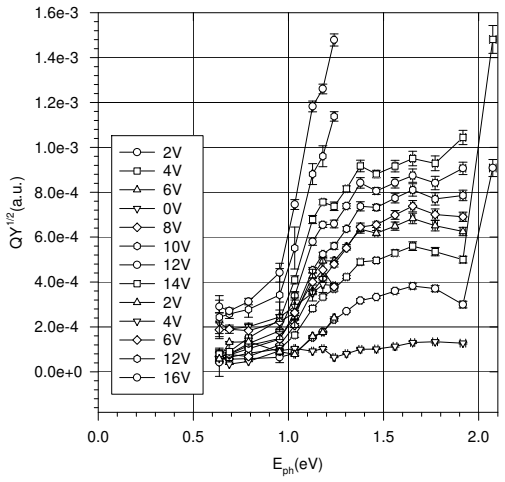

coward

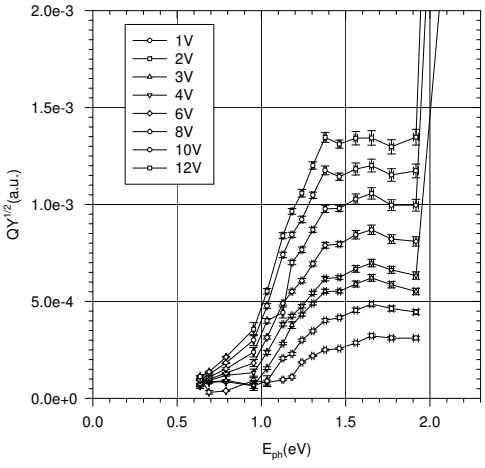

reverse

Figure 5.3: IPE-spectra of a Au/PPV/ITO sample.

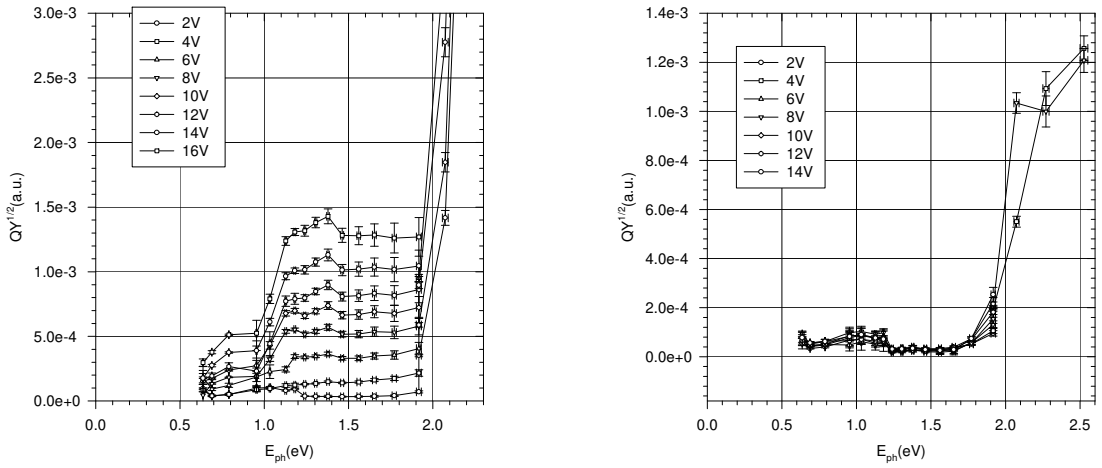

forward reverse

Figure 5.4: IPE-spectra of a Ca/PPV/ITO sample.

5.1.2 Ca/PPV/ITO

Characteristic IPE-spectra of Ca/PPV/ITO-samples are given in figure 5.4. As we can see, indeed a signal at photon-energies smaller then the band gap is measured in the forward. In earlier measurements by Rikken [63] a barrier for electrons was found of 0.6 eV. From modeling of the IV-curves a barrier of approximately 0.4 eV is expected [5]. If the Ca is biased negatively (forward bias) (so we collect injected electrons), the photo-current signal should therefore come up at photon-energies around this values. Biasing the sample in the reverse, holes rather then electrons will be collected and one measures the barrier-height for holes. The sum of these two should be the energy band gap in the polymer. As we see in the measurements, indeed a photo-current in the forward is detected, which comes up at approximately 0.7 eV. In the backward only some signal is seen around 1eV which is artificial, as is explained in section 4.4. Hole injection from the Ca contact should indeed only come up at a very high photon energy. No convincing barrier-lowering can be noticed, but *only* the Ca spectra do not contradict a photo-injection explanation.

We notice that a calcium device is a device with a asymmetric IV-curve. In the forward electrons from the Calcium and holes from the ITO-contact are flowing and in the backward the current is only small.

Samples with three different kinds of polymers were measured. One of them so called 'fully conjugated', indicating a high degree of purity, having longer fully conjugated strings in its molecules. Also different thicknesses, from 700 to 160 nm were used. Usually only the thicker ones produced showable results.

All of these measurements had a similar difference between forward and backward IPE-curves, but the 'shape' and magnitude varied somewhat.

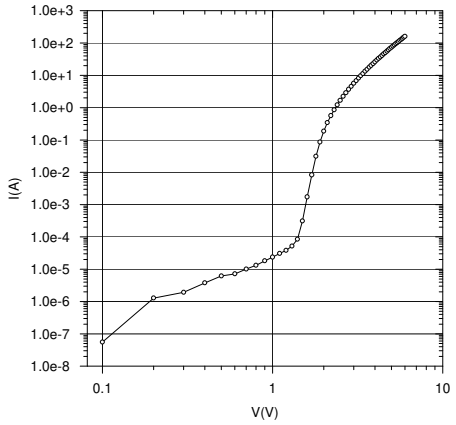

Figure 5.5: IV-curve of a Ca/PPV/ITO device

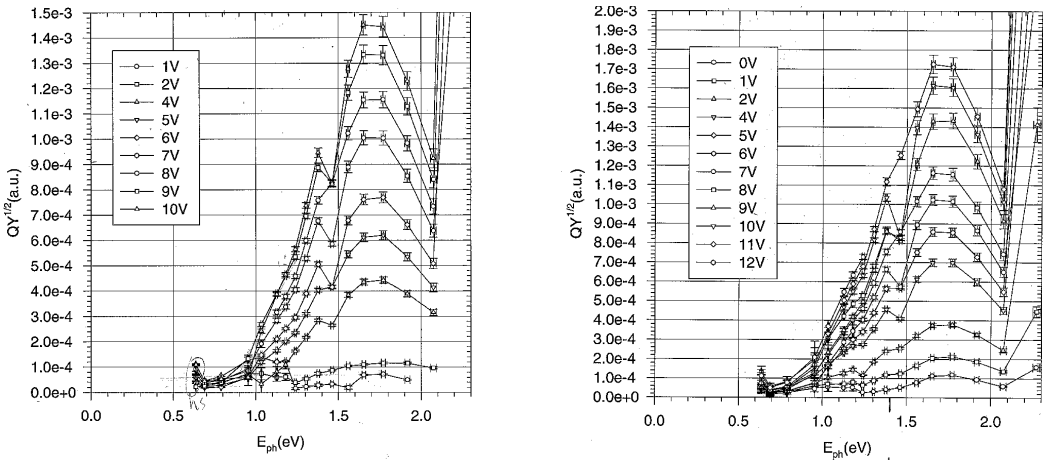

Figure 5.6: Spectrum of a indium/PPV/ITO sample

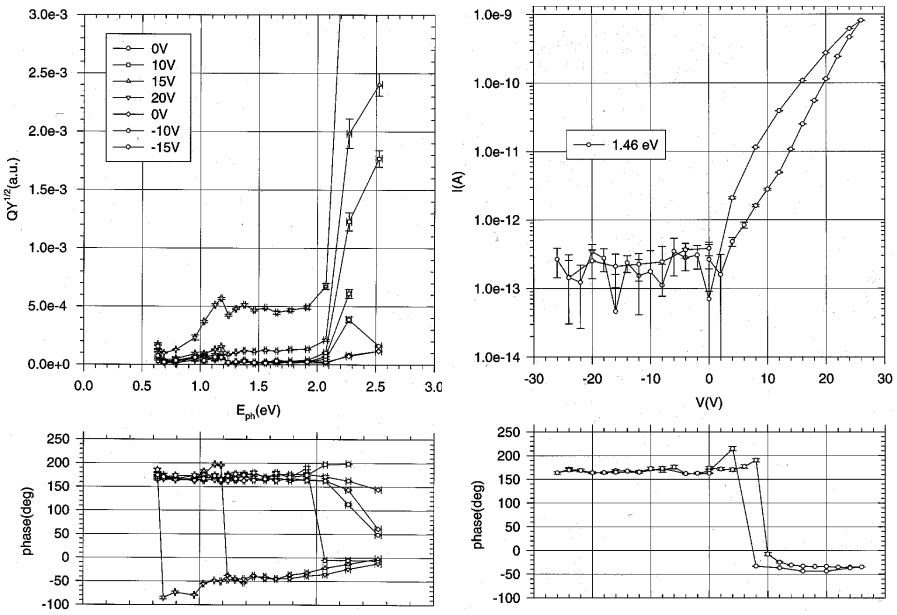

Figure 5.7: Spectra of a Al/PPV sample. The left picture are some spectra in forward and reverse voltages. In the right picture the dependence on the voltage on 1.46 eV was measured separately.

5.1.3 In/PPV/ITO

The spectra for the indium sample (figure 5.6) are even more 'beautiful' then the Au-spectra. These measurements are however difficult to interpret because the current was, comparing to 'normal' samples, much lower. They were also very symmetric, suggesting a ITO-like In-contact, also in contradiction to 'normal' samples. These samples are not reliable, but but further research might lead to the conclusion that this kind of samples are very well fit for photo-conductive observation of the polymer itself.

5.1.4 Al/PPV/ITO

The aluminum samples showed asymmetric behavior, as expected. An aluminum sample is supposed to be a 'hole-only' device in one direction and not to conduct in the other. This follows from the asymmetric IV-curves and the low luminescence, suggesting very few electrons in the forward. In the IPE-curves it showed very calcium-like behavior; sub-band-gap-photo-current when forward biased and nothing measurable in the backward. Spectra are given in figure 5.7. In this case forward and backward are given in one picture and an extra measurement of just the voltage dependence is given besides. We see that the voltage dependence is strong, and is comparable to the calculated results of chapter 3. But also we can remark that the voltage dependence is usually not very reproducible as is illustrated in this figure 5.7. The voltages was sweeped from 0 to 26 V and back and a clear hysteresis can be seen.

5.1.5 Explanation

In the IPE-spectra it seems to be the case that a below-band-gap-photo-current (BBG) is observed only if *holes* are flowing. Flowing electrons seem to have no or little effect on BBG-photo-current. Because of the similar behavior of the signal, when it occurs, independent of the expected barrier height which should be measured, concluded is that the signal is *not* a photo-injection current. This is in agreement with the fact that the IV-curves of samples with a hole-injecting contact (such as Au/PPV/ITO in both directions) can be well described by space-charge limited currents.

It must therefore be a bulk-effect. It only occured when holes were flowing, so an explanation must account for absence of the signal when there are not.

Empty hole-traps

If in the polymer occur traps for holes which are empty, it could explain the measured effect. If holes are flowing, the effective mobility of them would be lowered while part of them will be trapped. Illuminating the polymer, traps will be emptied, leading to an equilibrium with less trapped holes. The effective mobility will be higher and a bigger hole current will flow. When no holes are flowing, no holes will be trapped, so no can be untrapped either, therefore the signal will not increase then.

Because the signal comes up at 0.9 - 1 eV this must be about the depth of the traps (energy above valence-band in band-structure diagram). It then increases several tenths of an eV before it saturates or get lower again. This suggests that the width of this band plus the width of the valence band of the polymer is about this large.

Only empty hole-traps will also strongly influence the total dark current (make it a lot smaller).

Full hole-traps

Full hole traps will have the same effect, but they will also raise a current, when no holes are flowing. This no-hole-photo-current will however be time-dependent while the sample charges, and in steady state it will not be observed. Advantage from this explanation is that is will hardly influence the dark current. Therefore the explanation of full traps will be preferred.

It is possible that these full traps act as empty electron traps, but we assume the chance an electron traps in this kind of traps very small.

It is also possible to have empty hole traps, in which holes are only rarely trapped, but illuminating would than also have only little effect.

The voltage dependence of the IPE curves are normally approximately the same as the voltage dependence of the dark-IV curves, which is in good agreement with the numerical results.

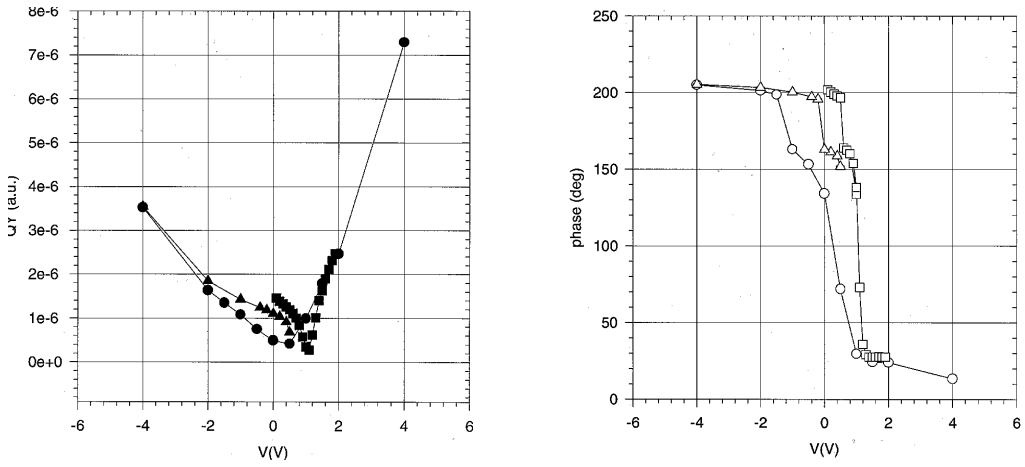

Figure 5.8: A build-in voltage measurement on a Ca/PPV(300 nm)/ITO-sample.

5.1.6 Reproducibility

IPE-spectra of sample reproduced normally their shape if the measurement was redone on the same sample. Reproducibility between sample often was limited to general effects.

5.2 Build in voltages

The build in voltage of a sample could be measured by illuminating the sample with above band gap light and measuring the photo-current as a function of the bias voltage. This build in voltages indicates the difference between barriers on the ITO and the metal.

For a Ca/PPV/ITO sample, a build-in voltage was measured to be around 1 ± 0.1V (see figure 5.8). Leading to a barrier of $E_{gap}/e - \Phi_{ITO} - 1 \approx 0.8$ eV, which is high.

These measurement turned out to be very irreproducible on different samples, and on the same (minima can even be at negative voltages as high as 15V!). Because nothing of interest can be conclude out of these measurement no further attention is given to them.

This kind of measurements were mostly used to observe the voltage dependence of the BBG-photo-conductivity. The voltages was then sweeped over a larger range [1].

5.3 Time dependence

Several measurements involving time-dependence were done, to get an idea of fastness of the processes and the influence of the chopping of them for the sake of the lock-in amplifier.

A general tendency was that the current steadily increases or decreases for hours. Switching on or off the light will disturb to sample for minutes, before reaching a new 'equilibrium'.

[1] for a simple Build-in voltage sweeping from 0 to 2 V should be sufficient anyhow

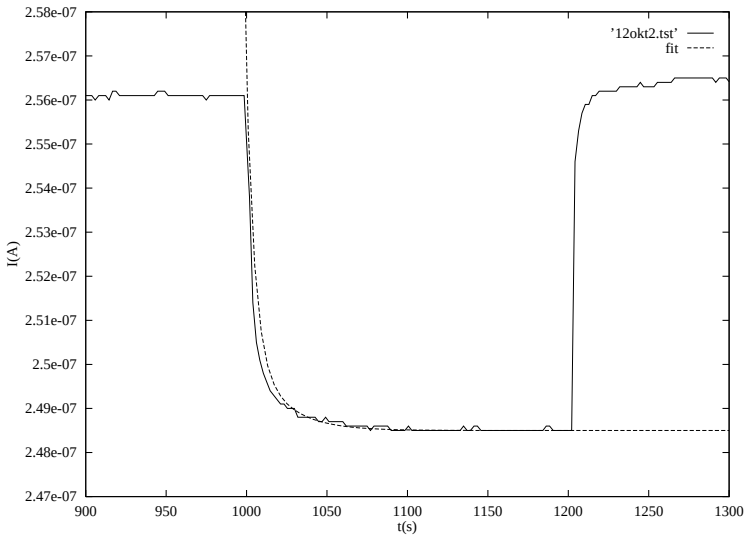

Figure 5.9: Time dependence of the illuminated (1.5 eV) current through a Al/PPV-sample, forward biased at 20 V.

Below band-gap photo-conductivity For a typical Au/PPV sample the current through the sample was measured, with an ordinary ammeter, as a function of time, while switching on and off the light (800 nm) every 200 seconds or so. Then the difference between a dark current and a illuminated current (I reserve 'photo-current' for the difference) is readily measurable. A measurement is given in figure 5.9. This effect is seen to be on a time-scale of tens of seconds.

If the signal is due to filling and unfilling of traps, as was assumed then one can with a theory for discharging of traps [44] say something about the trap-depth, using the time dependence of the photo-current.

$$j_{photo}(t) = -qp_t de_p \exp(-e_p t) + j_0 \tag{5.2}$$

So e_p can be found out of a measurement like in figure 5.9. e_p, the rate of hole emission, is related to the trap-depth E_t according to:

$$e_p = \nu_p \exp(-E_t/k_B T) \tag{5.3}$$

with ν_p the attempt-to-escape frequency, which is correlated with the light intensity, absorption and the phonon density (thermal detrapping). The temperature is low, while the trap depth is possibly $\approx$1 eV (as conclude from the photo-conduction spectra) so thermal detrapping can be ignored. The absorption is very low and not accurately known at this wavelengths (see [64]). The light intensity was about $2 \cdot 10^{16}$ photons /m^2/s, but this not very accurate because the constant c of formula 4.2 is poorly known.

In figure 5.9 a fit is drawn which consist of a sum of two exponentials, namely:

$$j_{photo}(t)_{fit} = 2.485 \cdot 10^{-7} + 0.06 \cdot 10^{-7} \exp(-(t-1000)/5) + 0.02 \cdot 10^{-7} \exp(-(t-1000)/20) \tag{5.4}$$

So two trap levels with values of e_p of 1/5 /s and 1/20/s were assumed. Probably a band of traps states would be best. A simple single level exponential function could not be fit satisfactory to the measured results.

From equation 5.2 something can be found for p_t:

$$p_t \approx \frac{0.06 \cdot 10^{-7}/\mathrm{s}}{qd0.2} = \frac{0.06 \cdot 10^{-7}/(3 \cdot 10^{-3})^2}{q \cdot 600 \cdot 10^{-9} \cdot 0.2} = 3 \cdot 10^{22}\ /\mathrm{m}^3 \tag{5.5}$$

which is a very reasonable answer.

5.4 IPE-spectra of T_{12}-samples

There were also taken some IPE-spectra from samples with thiophene-oligomer (T_{12}, see 2.2 for a structure formula of poly-thiophene, T_{12} is trivially similar.). T_{12} is of no interest for the PLED-project, but is meant to be used in organic diodes [42]. Samples were made by Erik-Jan Lous at Philips research laboratories, with practically the same structure as the PPV-samples. The metal contact was gold or tin. A doped and undoped (at least not intentional) variant of thiophene was used. T_{12} has a band-gap of approximately 2.3 eV. The absorption-coefficient in T_{12} is much bigger then in PPV, so it is expected that a sample is not uniformly illuminated.

Spectra are shown in figure 5.10. They show a photo-current behavior similar to the PPV-samples. The valence/conduction band photo conductivity should come up at about 2.3 eV, according to absorption measurements. The signal is not, like in the PPV-samples, dramaticly increasing, but decreasing here. This is due to the large absorption. The limiting insulating layer [38] near to the metal/oligomer contact is not illuminated anymore then, leading to a decrease in photo-current.

We see a clear difference in BBG-photo-conductivity between unintentionally and intentionally doped oligomer samples, indicating that the signal has something to do with the doping level, supporting the idea that the increase in photo-conductivity is due to gap states.

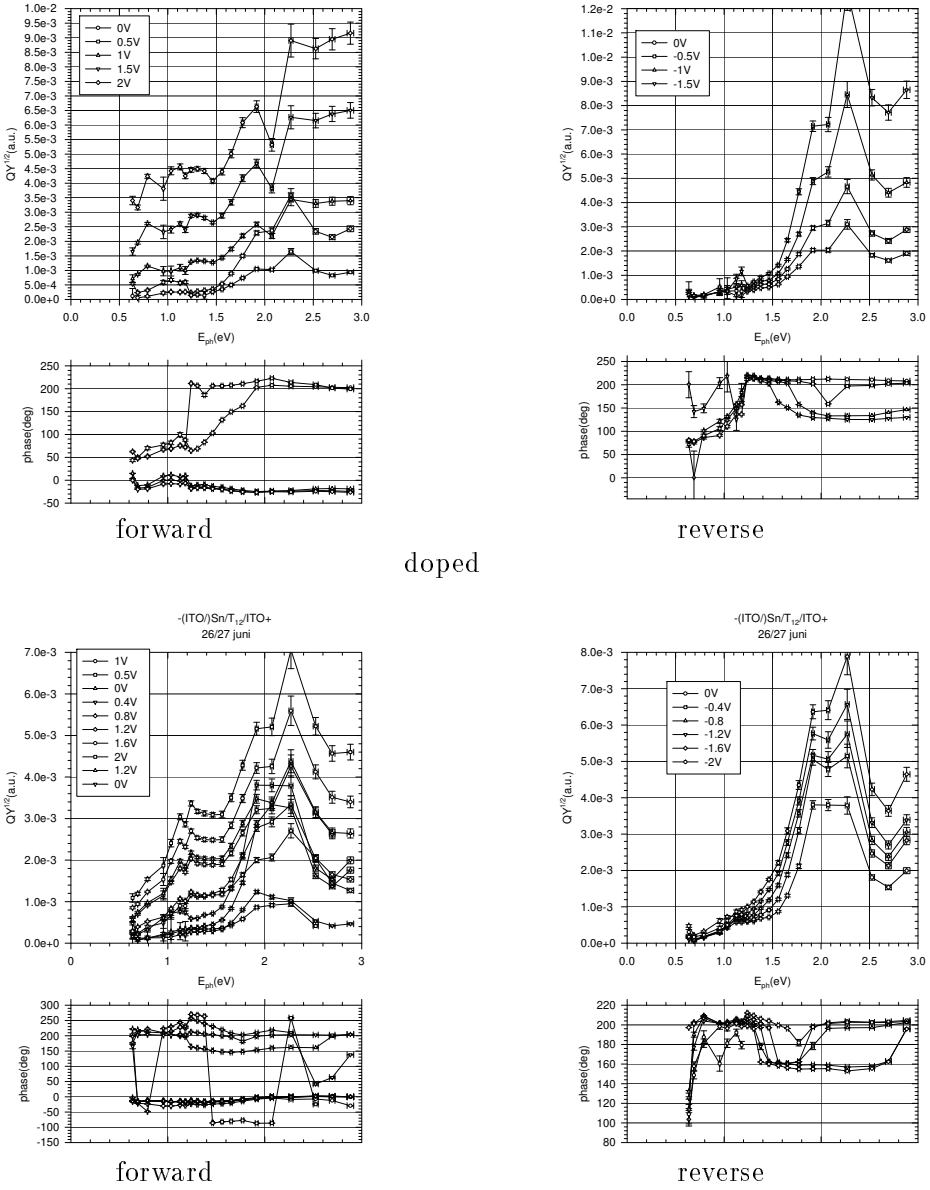

Figure 5.10: Spectra of $Sn/T_{12}/ITO$ samples

Chapter 6

Conclusions

We can conclude that the polymers under study have a very low mobility, and therefore the IV-curves of a Poly-LED is strongly limited by space charge if the barrier-height is small (as in the electron-injecting Ca/PPV-samples, and certainly at the hole-injecting Au/PPV-contact). These small barrier heights therefore cannot be measured using a photo-injection technique, because extra injected electrons will have no effect on the total current. The signal seen was due to the polymer itself, which was photo-conducting below the bandgap somewhat. During the time of this measurements relatively thick samples were used, and only the thickest (700 nm) gave presentable results. If the characteristics of thinner samples (<100 nm) becomes better (more reliable IV-curves) possibly photo-injection can be a technique to determine high barriers for electrons of e.g. In/PPV and Al/PPV contacts. The bulk absorption is then smaller (thin layer) and the current less or not space charge limited (higher barriers).

The photo-current below bandgap, which was observed, is likely to be due to traps for holes in the polymer. Holes are released from these traps when illuminating with the infra-red light, and the effective mobility of the bulk increases, thus given rise to a larger current. These traps were likely to be full, because this will not influence the dark current, but it was demonstrated numerically that it can induce this BBG-photo-conductivity.

A photo-conductive technique as was described can be used to obtain informations about traps in the bulk of the polymer. However the use of a LIA better is avoided because the illumination should be chopped and one can be sure that steady state never will be reached (a 'steady state' is reached only after 100 seconds or so, as can be seen in figure 5.9). This makes it difficult to make a proper comparison with theoretical calculations. However it may be possible to take into account the chop-frequency in the calculations, but this was not done.

Simple time-dependence measurements, combined with photon-energy-dependency measurements as 'IPE-spectra' may eventually lead to more informative methods of estimating the trap-depths and density of the bulk of the polymer. One should remember that in experiments at the bulk-conduction-properties of polymers, the conduction should be limited by the bulk, and not by the contact, and the barriers on the interface should therefore be low. For the polymers studied, an interface with ITO will be low enough, and also gold will do. If one want study the photo-conductive properties of *electrons* one should use a

good electron injecting contact, together with a non-injecting hole contact. One of the contacts should be transparent, to be able to illuminated the bulk. Calcium may have a low enough work-function, but we cannot be sure because electron-only samples were not studied yet at the time of this research.

One could also think of so called dual beam photo-conductivity [75]. The below band gap photo-current is measured in the same way as described, but the sample is also illuminated with light having a small wavelength. The sample is continuously photo-excited then and a large photo-current will flow. In this way also the real photo-current could be observed in a controlled way, because the total number of free carriers stays the same (see [75]).

It is possible that the below band gap photo-current measured in such a dual beam experiment reaches faster a steady state, making it possible to make more reliable 'IPE'-spectra. In this manner we also can make sure that electrons are flowing in a otherwise hole-only device. This was tried with an extra Hg-lamp on a Al/KTB 26/ITO sample and it resulted in much higher signals, but not of a different shape in the forward direction. Enforcing the suggestion that only the presence of holes is of influence on the below band gap photo-current. The signal became a lot 'noisier' in some cases, of which the cause was not found yet.

Bibliography

[1] JM André, LA Burke, J Delhalle, G Nicolas, Ph Durand – Int. J. Quantum Chem.: Quantum Chem. Symp. **13** (1979) 283

[2] H Antoniadis, *et al* – Synth. Met. **62** (1994) 265

[3] BG Bagley – Solid State. Commun. **8** (1970) 345

[4] J Bardeen – Phys. Rev. **71** (1947) 717

[5] PWM Blom – *Personal communication* – 1995

[6] PWM Blom – *to be published* – IEDM 1995 proceedings

[7] DF Blossey – Phys. Rev. B **9** (1974) 5183

[8] DDC Bradley, RH Friend, H Lindenberger, S Roth – Polymer **27** (1986) 1709

[9] DDC Bradley, RH Friend, WJ Feast – Synth. Met. **17** (1987) 645

[10] D Braun, AJ Heeger – Appl. Phys. Lett. **58** (1991) 1982

[11] AR Brown, K Pichler, NC Greenham, DDC Bradley, RH Friend, AB Holmes – Chem. Phys. Letters **210** (1993) 61

[12] RL Burden, JD Faires – *Numerical Analysis, fourth edition, chapter 2* – PWS-Kent, Boston, 1989

[13] JH Burroughes, *et al* – Nature **347** (1990) 539

[14] RF Chaiken, DR Kearns – J. Chem. Phys. **45** (1966) 3966

[15] NF Colaneri, DDC Bradley, RH Friend, PL Burn, AB Holmes, CW Spangler – Phys. Rev. B **42** (1990 II) 11670

[16] CR Crowell, WG Spitzer, LE Howardth, EE LaBate – Phys. Rev **127** (1962) 2006

[17] CR Crowell, SM Sze – Solid-State Electron. **9** (1966) 1035

[18] EG&G – *A Lock-In Primer* – EG&G Princeton Applied Research, Princeton, 1986

[19] DE Eastman – Solid State. Commun. **8** (1970) 41

[20] DJ Fabian, LM Watson (editors) – *Band Structure Spectroscopy of Metals and Alloys* – Academic Press, London, 1974

[21] RH Fowler – Phys. Rev. **38** (1931) 45

[22] RH Friend, DDC Bradley, PD Townsend – J. Phys. D: Appl. Phys. **20** (1987) 1367

[23] OM Gelsen, *et al* – Mol. Cryst. Liq. Cryst. **216** (1992) 117

[24] NC Greenham, SC Moratti, DDC Bradley, RH Friend, AB Holmes – Nature **365** (1993) 628

[25] Y Greenwald, *et al* – Synth. Met. **69** (1995) 365

[26] AJ Heeger, ID Parker, Y Yang – Synth. Met. **67** (1994) 23

[27] V Hernández, Navarrete, JT Lópe – Synth. Met. **51** (1992) 211

[28] M Hubin, J Gouault – C. R. Acad. Sc. Paris B **275** (1972) 195

[29] Mitsusuke Ikeda – J. Phys. Soc. Japan **45** (1978) 247

[30] J Jackson – *Classical Electrodynamics, second edition* – John Wiley & Sons

[31] H Kanter – Phys. Rev. B **1** (1970) 522

[32] C Kittel – *Introduction to Solid State Physics, sixth edition* – John Wiley & Sons, New York, 1986

[33] WF Krolikowski, WE Spicer – Phys. Rev. **185** (1969) 882

[34] H Kruis, M Meeuwissen – *Dataacquisitie; Metingen gedaan met een computer* – D-practicum-verslag, Universiteit Utrecht, 1994

[35] AI Lakatos, J Mort – Phys. Rev. Lett. **21** (1968) 1445

[36] CH Lee, *et al* – Mol. Cryst. Liq. Cryst. **256** (1994) 745

[37] CH Lee, G Yu, D Moses, AJ Heeger – Phys. Rev. B **49** (1994) 2396

[38] DM de Leeuw, EJ Lous – Synth. Met. **65** (1994) 45

[39] M Lenzlinger, EH Snow – J. Appl. Phys. **40** (1069) 278

[40] J Levinson, Z Burshtein, A Man – Mol. Cryst. Liq. Cryst. **26** (1974) 329

[41] Lögdlund, *et al* – Synth. Met. **41-43** (1991) 1315

[42] EJ Lous, PWM Blom, LW Molenkamp, DM de Leeuw – Phys. Rev. B **51** (1995) 17251

[43] A Many, J Levinson, I Teucher – Mol. Cryst. **5** (1969) 273

[44] Hideharu Matsuura, Masahiro Yoshimoto, Horoyuki Matsunami – Jpn. J. Appl. Phys. **34** (1995). L185

[45] H Mayer, H Thomas – Zeit. Phys. **147** (1957) 419

[46] CA Mead – Solid-St. Electron. **9** (1966) 1023

[47] CA Mead, WG Spitzer – Phys. Rev. **134A** (1964) 173

[48] M Meeuwissen, *et al* – *Measurement program for 'IPE'-measurements* – Philips Research, Eindhoven, 1995

[49] M Meeuwissen, PWM Blom – *Numerical program for photoIV-curves* – Philips Research, Eindhoven, 1995

[50] AG Milnes, DL Feucht – *Heterojunctions and Metal-Semiconductor Junctions* – Academic Press, New York, 1972

[51] J Mort, FW Schmidlin, AI Lakatos – J. Appl. Phys. **42** (1971) 5761

[52] J Mort, AI Lakatos – J. Non-Cryst. Sol. **4** (1970) 117

[53] J Mort, DM Pai (editors) – *Photocunductivity and Related Phenomena* – Elsevier Scientific Publishing Company, Amsterdam, 1976

[54] G Nicolas, Ph Durand – J. Chem. Phys. **70** (1979) 2020

[55] ID Parker – J. Appl Phys. **75** (1994) 1656

[56] E Passaglia (editor) – *Techniques of metals research volume VI, Measurements of Physical Properties part 1* – Interscience Publishers, New York, 1972

[57] AV Patsis, DA Seanor (editors) – *Photoconductivity in Polymers* – Technomic Publishing Co., Westport, 1976

[58] M Pollak, B Shklovskii (editors) – *Hopping Transport in Solids, chapter 11 by S. Roth* – North-Holland, Amsterdam, 1991

[59] U Rauscher, H Bässler, DDC Bradley, M Hennecke – Phys. Rev. B **42** (1990) 9830

[60] P Rénucci, L Gaudart, JP Pétrakian, D Roux – Thin Solid Films **89** (1982) 27

[61] PJ Reucroft, SK Ghosh – Phys. Rev. B **8** (1973) 803

[62] PJ Reucroft, H Scott, FL Serafin – J. Polymer Sci. C **30** (1970) 261

[63] GLJA Rikken, YARR Kessener, D Braun, EGJ Staring, R Demandt – Synth. Met. (**1994**)

[64] STR Romme – *Photochemical stability of Polymers used in* LEDs – Philips Research, 1995

[65] WR Salaneck, JL Brédas – Synth. Met. **67** (1994) 15

[66] W Shockley – Phys. Rev. **56** (1939) 317

[67] B Stolecki, A Borodziuk-Kulpa, C Wesolowska – Thin Solid Films **116** (1984) 317

[68] WP Su, JR Schrieffer, AJ Heeger – Phys. Rev. B **22** (1980) 2099

[69] LS Swanson, *et al* – Phys. Rev. B **46** (1992-I) 15072

[70] SM Sze, CR Crowell, D Kahng – J. Appl. Phys. **35** (1964) 2534

[71] SM Sze, JL Moll, T Sugano – Solid-St. Electron. **7** (1964) 509

[72] SM Sze – *Physics of Semiconductor Devices, second edition* – John Wiley & Sons, New York, 1981

[73] Akio Takimoto, Hisahito Ogawa – J. Photopol. Sci. Technol. **6** (1993) 171

[74] J Vancea, H Hoffmann, K Kastner – Thin Solid Films **121** (1984) 201

[75] MJWM van de Ven – *Optical Characterisation of Thin Film Silicon Alloys* – Master Thesis: VDF/NG 94-13, Eindhoven, 1994

[76] IA Vermeulen, HJ Wintle – J. Polymer Sci. A**2** 8 (1970) 2187

[77] R Williams, RH Bube – J. Appl. Phys. **31** (1960) 968

[78] R Williams, J Dresner – J. Chem. Phys. **46** (1967) 2133

[79] Wei-Kang Wu, S Kivelson – Phys. Rev. B **33** (1986) 8546

[80] Y Yang, AJ Heeger – Appl. Phys. Lett. **64** (1994) 1245

[81] KE Ziemelis, *et al* – Phys. Rev. Lett. **66** (1991) 2231

Appendix A

The numerical program

The program for numerically understand a sample which is illuminated is given below. It was written in C++ and inspired by the programs Paul Blom wrote in Turbo Pascal. The program uses the header-file 'numerical.h' which was written to calculate the inverse of a function in a certain point and is given after the main-program.

It also uses the header-file 'big.h'. This offers the use of the 'bigfloat' type. This type is like a double, but is secured against overflow runtime errors. At the computer system used at Philips Research this was not necessary, but for the system of the Utrecht physics department it's essential. This is because the use of the inverse functions of 'numeric.h' can use a very 'bad' initial approximation giving rise to absurdly large results in the first steps of the procedure.

All mentioned files ('ipesclc.cpp', 'numeric.h' and 'big.h' can be obtained from the author (meeuwiss@fys.ruu.nl)).

The heart of the program 'sclcipe.cpp' are the functions `float fie (floatt)`, `floatt Vappr(floatt)` and `Jappr(floatt)`, which are given below. A program is supposed to be self-explanatory, so no further commence is given here:

```
.. omitted a lot.....

// of er licht is en of het invloed heeft:
boolean licht = (boolean)(( (Nth>0) || (Nte>0)) && (cill>0));

//---------------------------------------------------------------------------
inline floatt Nh(floatt c=0)      {return (Nvh*(exp(-Eth*eDkBT)+c)); }
inline floatt Ne(floatt c=0)      {return (Nce*(exp(-Ete*eDkBT)+c)); }
// FD voor traps en HB voor VB}

inline floatt ntfun(floatt n,floatt c=0)    {return 0; /* Nte*pow(n/Nce,D1);*/ }
inline floatt ptfun(floatt p,floatt c=0)    {return Nth/(1+Nh(c)/p); }

inline floatt recombination(floatt n, floatt p) {return n*p*(R+1/(tau*(n+p)));}

inline floatt cx(floatt xx)
{ switch(direction)
  { case holecont      : return(s.c*exp(-xx/lambda));
    case electroncont  : return(s.c*exp(-(d-xx)/lambda));
    default            : return(s.c);
  }
}
// field dependent mobility:
inline floatt emueE(floatt E)    {return emue0Dalfae*sinh(alfae*E); }
inline floatt emuhE(floatt E)    {return emuh0Dalfah*sinh(alfah*E); }

// quasi fermi level (given by the inverse FD-function)
inline floatt imref(floatt np,floatt Ncv)      { return kBT*log(Ncv/np -1); }

// functions at a Schottky contact (SC)
// SC barrier lowering
```

```
inline floatt DeltaFi(floatt E) { return  sqrt(abs(eDeps*E/(4*pi)));}
//carrier density at a SC (thermal)
inline floatt carriercontact(floatt E, floatt Fi, floatt Ncv)
      { floatt fi=Fi-DeltaFi(E); if (fi<0) fi=0;
        return Ncv/(1+exp(fi*eDkBT)); //FD  }
//current at the hole injecting SC, as a function of the electrical field.
//  and given s.n[0]
inline floatt hcontactJ(floatt E)
      {   return  carriercontact(E,Fih,Nvh) * emuhE(E) + s.n[0] * emueE(E); }

//SC barrierheight at the electron injecting SC (an inverse of 'carriercontact').
inline floatt fifun(floatt E, floatt n)
      { if (n<0) return 100;
        else if (n>Nce/2) return 0;
        else return(  kBTDe* log (Nce / n -1)
                    + DeltaFi(E)                  );
      }

// inner loop: find fie as a function of n[x=0]
floatt fie(floatt nx0)
{  float decx;
  s.n[0]  = nx0;
  s.E[0]  = inverseinc(hcontactJ,s.I,apprvars(0,1e8)).value;
  s.p[0]  = carriercontact(s.E[0],Fih,Nvh);   // tweede keer, maar ja

  decx=cx(0);
  s.nt[0] = ntfun(s.n[0],decx);
  s.pt[0] = ptfun(s.p[0],decx);

//pt0[0] p0[0] nt0[0] n0[0] can be replaced by pt00 p00 nt00 n00 if no light or no absorbtion
  s.pt0[0] = (s.somh + Nh(decx) + Nth - sqrt( sqr(s.somh+Nh(decx)+Nth) - 4*s.somh*Nth))/2;
  s.p0[0]  = s.somh - s.pt0[0];

  s.nt0[0] = (s.some + Ne(decx) + Nte - sqrt( sqr(s.some+Ne(decx)+Nte) - 4*s.some*Nte))/2;
  s.n0[0]  = s.some - s.nt0[0];

  s.Ea[0] = eDeps * (s.p[0]  - s.p0[0] + s.pt[0]  - s.pt0[0]
                   - s.n[0]  + s.n0[0] - s.nt[0]  + s.nt0[0] );
  s.dx[0] = min(dxfac * abs(s.E[0]/s.Ea[0])+minstep,maxstep);

  s.x[0]  = 0;
  s.je[0] = s.n[0]*emueE(s.E[0]);
  s.jh[0] = s.p[0]*emuhE(s.E[0]);
  s.jsl[0]= e*recombination(s.n[0],s.p[0]);
  s.licht = R*s.n[0]*s.p[0]*s.dx[0];

  floatt vtot=s.E[0]*s.dx[0];

  s.warningi=' ';
  unsigned i=0;
  while(s.x[i]<d)
    { i++;
      if (i>=(maxnstep-1)) {s.x[i-1]=d; s.warningi='@';}
      s.E[i]   = s.E[i-1]  + s.dx[i-1]*s.Ea[i-1];
      if (s.E[i]<0) {s.nstep=i; s.n[i]=Nce/2;
                     s.warningi='E';
                     s.V=vtot;
                     s.foundFie=0; // fifun(s.E[i],s.n[i])
                     return s.foundFie;
                    }
      s.je[i]  = s.je[i-1] + s.dx[i-1]*s.jsl[i-1];
      s.jh[i]  = s.jh[i-1] - s.dx[i-1]*s.jsl[i-1];

      s.x[i]   = s.x[i-1] + s.dx[i-1];
      decx     = cx(s.x[i]);

//    pt0[i] p0[i] nt0[i] n0[i] can be replaced by pt00 p00 nt00 n00 if no light or no absorbtion
      s.pt0[i] = (s.somh + Nh(decx) + Nth - sqrt( sqr(s.somh+Nh(decx)+Nth) - 4*s.somh*Nth))/2;
      s.p0[i]  = s.somh - s.pt0[i];

      s.nt0[i] = (s.some + Ne(decx) + Nte - sqrt( sqr(s.some+Ne(decx)+Nte) - 4*s.some*Nte))/2;
      s.n0[i]  = s.some - s.nt0[i];

      s.p[i]   = s.jh[i] / emuhE(s.E[i]);
//    if (s.p[i]>Nvh) s.p[i]=Nvh;  // p[i]<= Nvh  current?!
      if (s.p[i]<0) s.p[i]=0;
      s.pt[i]  = ptfun(s.p[i],decx);
      s.n[i]   = s.je[i] / emueE(s.E[i]);
//    if (s.n[i]>Nce) s.n[i]=Nce;  // n[i]<= Nce
      if (s.n[i]<0) s.n[i]=0;
      s.nt[i]  = ntfun(s.n[i],decx);

      s.Ea[i]  = eDeps * (  s.p[i] - s.p0[i] + s.pt[i]  - s.pt0[i]
                          - s.n[i] + s.n0[i] - s.nt[i]  + s.nt0[i] );
      s.dx[i]  = min(dxfac * abs(s.E[i]/s.Ea[i])+minstep,maxstep);

      s.jsl[i] = e*recombination(s.n[i],s.p[i]);
      s.licht += R*s.n[i]*s.p[i]*s.dx[i-1];
      vtot    += s.E[i]*s.dx[i-1];
    }
  s.nstep=i;
```

```
  s.V=vtot;
  s.foundFie= fifun(s.E[s.nstep],s.n[s.nstep]);
  return s.foundFie;
}

floatt Vappr(floatt j)
 { result invresult;
   s.I=j;
   // inner loop: warnings op nul zetten:
   s.warningi=' ';
   s.warningn=' ';

if (doublecarrier)
  { invresult=inversedec(fie,Fie,apprvars(1e-300, 1   , 1e-5,300,logBS));
   //                                          Nce
   if (invresult.warning) s.warningn='!';
   // NR gaat hier fout, als lowerlim=0 in elk geval.
   s.denx0=invresult.value;
  }
else
 {// 1 carrier (just holes):
   fie(0);
   s.denx0=0;
 }
return s.V;
 }

floatt Jappr(void)
 { result invresult;
   // find or don't find V (commence one out)
   // find V:
   invresult=inverseinc(Vappr,s.V,apprvars(1e-9,1e5,1e-5,200,logBS));
   if (invresult.warning) printf("%");
   // if something is wrong in last inner loop: warning!
   if (s.warningi!=' ') printf("%c",s.warningi);
   if (s.warningn!=' ') printf("%c",s.warningn);
   return invresult.value;
   /*
   // don't find V:
   s.V=Vappr(s.I);
   return s.I;
   */
 }

.... A suggestion for solving the problem with diffusion. time solved simulation of sample ....omitted.....

//-------one carrier functions (for comparision)-------
floatt Johm(floatt V,floatt p0) { return(area*p0*emueE(V/d)); }
// geen SCL effecten, slechts mu=mu(E)=mu(V)
inline floatt Vscl(floatt j)    { floatt g=sqr(alfah)*j/(eps0*epsr*mue0);
                                  return (((g*d +1)*acosh(g*d+1) -sqrt(g*d*(2+g*d)))/(alfah*g));
                                }
floatt Jscl(floatt V)           { return(area*inverseincNR(Vscl,V,apprvars(1e-6,1e6,1e-5,100)).value); }
inline floatt Jsclmu(floatt V)  { return(area*9/8*mue0*epsr*eps0*V*V/(d*d*d));}

.. omitted...
main()
{..omitted...
calls the above functions e.g. like this:
        s.V=V
        s.c=cnoill;
        printf("%e   ",double(Jnoill=Jappr()));

}
//einde hoofprogramma-------------------------------------------------------------------------------
... implementation of some I/O routines omitted.....
```

numerical.h

The following header file contains the functions to numerically inverse a function. It contains a Newton-Raphson algorithm ('Secant' algorithm) which uses initial values from a bisection algorithm (see also [12])

```
// numeric.h
// Hichiel Heeuwissen - oktober 1995
// Philips Research Laboratories Eindhoven
floatt abs(floatt x) {return x<0 ? -x : x}
// Numerical inverse of a user defined function

// Bisection choosers logBS or simpleBS
/*  logBS costs a sqrt, but needs a lot less iterations if minx and maxx are very badly chosen. It will need slightly more otherwise.  Disadvantage of logBS: min an m
inline floatt simpleBS(floatt min, floatt max) {return (min+max)/2; } // simply take new value exactly between two extremes
inline floatt logBS   (floatt min, floatt max) { return sqrt(min*max); } // take new value exactly between two extremes on a logarithmic scale
class apprvars {public:
              apprvars(floatt mi=0,floatt ma=100, floatt t=1e-15,unsigned m=100, floatt bsf(floatt,floatt)=simpleBS)
```

```
               { lowlimit=mi; uplimit=ma;
                 tolerance=t; maxnit=m;
                 BS=bsf;
                }
             floatt   tolerance;// iteration relative tolerance
             unsigned maxnit;   // maximum number of iterations
             floatt   lowlimit; // most approximations need a lower and upper limit
             floatt   uplimit;
             floatt  (*BS)(floatt, floatt);
            };
class result{ public:
             result(unsigned n=0, floatt min=0, floatt max=1, floatt val=0, int w=0)
                  { nit=n; minx=min; maxx=max; value=val; warning=w;}
             unsigned nit;
             floatt maxx,minx;
             floatt value;
             int warning;
           };
/* ------------------------------------------------------------------------
  Bisection-algorithm based inverses. */
// Inverse of a monotonic increasing function:
inline result inverseinc(floatt f(floatt),floatt y,apprvars a);

// Inverse of a monotonic decreasing function:
inline result inversedec(floatt f(floatt),floatt y,apprvars a);

// Inverse of a monotonic function (Use only when borders can be filled in):
inline result inverse(floatt f(floatt),floatt y, apprvars a);
// Completely automatic version, can be slow and give problems (borders are first guessed to be 0 and 100 and are eventually changed:)
inline result inverse(floatt f(floatt),floatt y);
//------------------------------------------------------------------------
// Newton-Raphson based inverses (Secant algorithm).
// NR: inverse using the result of BS inverse function bs:
inline result NR(floatt f(floatt), floatt y, result bs, apprvars a);

// inverse??NR use the BS inverse??-functions until bsNRprec is satisfied,
// completing it with the NR-function
floatt bsNRprec=0.1;  // tot 10% met bisectie
inline result inverseincNR(floatt f(floatt), floatt y, apprvars a);
inline result inversedecNR(floatt f(floatt), floatt y, apprvars a);
inline result inverseNR(floatt f(floatt), floatt y, apprvars a);
inline result inverseNR(floatt f(floatt), floatt y);
/* ------------------------------------------------------------------------
   general:
 Host 'inverse'-functions should be used with a argument of the type apprvars. Handy is it, to use the constructor e.g.:
 inverseinc(fun,y,apprvars(min,max));  // lower en upper limit are specified
                                       // tolerance and maxnit are default;
 inverseinc(fun,y,apprvars());         // everything is default
 inverseinc(fun,y,apprvars(min,max,1e-5,50)); // a tolerance of 1e-5 is spec. and maxnit of 50 */
/* ------------------------------------------------------------------------
      IMPLEHENTATION ..... omitted.....
```

Appendix B

The measurement program

The measurement program is a program written in Turbo Pascal which controlled the personal computer in the setup. It can measure a lot of relationships between measurable quantities, such as $\sqrt{QY}$ vs E_{photon} (Fowler Plots), photocurrent vs voltage, IV-curves and several quantities vs time. Other measurement-procedures can be added readily.

The most complex and most used procedure was the measuring of the photo-current using the LIA. This procedure, and other most important parts of the program are given below. This also has to perform the duties of a description of the way measurements were carried out excactly. The programs uses the type 'meetpunt' which can be seen as a floating point variabel with an error (It was described in [34]).

```
program measure;
 res=500
 resptime=40000
....omitted a lot.......
{-------------------------------------------------------------------------}
{-----measurement of QY--------------------------------------------------}

FUNCTION Overload : byte;
...omitted.........
{---functions for 'eval functions'-----}
 function hoek(x,y:double):double;far;
   ... similar to ...arctan y/x.....
 function lengteverschil(r,phi:double):double;far;
 begin lengteverschil:=sqrt(abs(r*r + sigzero.w*sigzero.w - 2*r*sigzero.w* cos((phasezero.w-phi)/180*Pi) ))  end;
{----}
Procedure HeasPhotoCurrent(var sigout,phaseout,refout:meetpunt);
VAR SumRef,SumRefsq, Refer   : Double;
    mag,phase,SigX,SigY,SumX,SumY: Double;
    totphase                 : meetpunt;
    sumxsq,sumysq            : double;
    x,y                      : meetpunt;
    sig                      : meetpunt;
               {mag:    grootte van het signaal gebruikt tijdens het meten
                sig:    grootte van het signaal zonder nulpuntcorrectie
                sigout: met nulpuntcorrectie
               }
    lijst                    : meetpuntlijst;
    .. some declarations omitted....
BEGIN
  ...
  SumRef:= 0;  sumrefsq:=0;
  SumX := 0; sumxsq:=0;
  SumY := 0; sumysq:=0;

  NISend(K485,'ROTOG1X',HsgX,HsgY);
  NISend(EGG5206,eggstring,HsgX,HsgY);
  delay(res);
  NISend(EGG5206,'S',msgx,msgy);  {verzoek om sens}
  delay(res);
  nireceive(egg5206,dumstr,msgx,msgy);
  val(dumstr,LockSensCode,errcd); {anders gewoon  := 17}
  { logout('egg5206'+eggstring+'     S:'+stri(locksenscode));}
  LockSens := Convert[LockSensCode];
  delay(res);
  niSend(EGG5206,'Z',msgx,msgy);
  delay(res);
```

```
nireceive(egg5206,dumstr,msgx,msgy);
val(dumstr,load,errcd);
if (load and 8) = 8 then
   begin
   message(msgx,msgy,'Reference low, check chopper <enter>');
   repeat ch:=break;
   until ch=enter;
   end;
OKHeas:=True;
wachtms(resptime div 2,msgx,msgy,break);
load:=overload;
WHILE (load>0) AND OKHeas DO BEGIN
 If LockSensCode>0 Then begin
    LockSensCode:=LockSensCode-1;
    LockSens := Convert[LockSensCode];
    Delay(Res);
    Str(LockSensCode,CodeString);
    Str(locksens:5,senssstring);
    dumstr:='';
    if (load and 1) = 1 then dumstr:=dumstr+'ch2 ';
    if (load and 2) = 2 then dumstr:=dumstr+'ch1 ';
    if (load and 4) = 4 then dumstr:=dumstr+'signal';
    Hessage(HsgX,HsgY-1,'Overload! ('+dumstr+') Changing Lock-in sens. to '+CodeString+' ('+senssstring+' V)');
    logout('OL! ('+dumstr+') LIA sens. to '+CodeString);
    NISend(EGG5206,'S '+CodeString,1,5);
    if (load and 4) = 4 then wachtsec(5,msgx,msgy,break)   {bij een signal overload hoeftie niet zo lang te wachten}
                        else wachtms(RespTime,msgx,msgy,break);
    Hessage(HsgX,HsgY-1,'');
    if keypressed then ch:=break;
    load:=overload
  end else OKHeas:=False;
END;

if keypressed then ch:=break;

Delay(Res);
If OKHeas Then begin
  wachtms(Round(RespTime/2),msgx,msgy,break);
  n := 0;
  if LockSens>0 then
  AvNum := Round(Abs(LN(LockSens)/2.31))*HulFac + 5
  else Avnum :=5;
  FOR i := 1 TO AvNum DO
    BEGIN
    infostring:='sens.:'+strd(locksens,1)+' V  \='+strd(lambda,3)+' nm';

    delay(3*Res);

    Hessage(HsgX,HsgY,stri(avnum-i)+' Sending command to EG&G...');
    NISend(EGG5206,'Q1;Q2',10,1);
    {ontvang channel 1 en channel 2}

    Hessage(HsgX,HsgY,stri(avnum-i)+' Reading reference...');
    NIReceive(K485,DumStr,1,20);
    Val(DumStr,Refer,ErrCd);

    delay(res);

    Hessage(HsgX,HsgY,stri(avnum-i)+' Reading magnitude...');
    NIReceive(EGG5206,Dumstr,10,2);
    Val(DumStr,Hag,ErrCd);
    Hag := Hag/2000*LockSens*PreSens*PAFac;

    Delay(Res);

    Hessage(HsgX,HsgY,stri(avnum-i)+' Reading phase...');
    NIReceive(EGG5206,DumStr,10,4);
    Val(DumStr,Phase,ErrCd);
    phase := phase/2000*pi;  {phase in radialen}

    gotoxy(msgx,msgy+1);
    write('ref:'+strd(refer,5)+'A   mag:'+strd(mag,5)+'A   phase:'+strd(phase*180/pi,5)+'deg    ');
      SigX     := Hag*COS(Phase);
      SigY     := Hag*SIN(Phase);
      SumX     := SumX + SigX;
      SumY     := SumY + SigY;
      sumxsq   := sumxsq + sigx*sigx;
      sumysq   := sumysq + sigy*sigy;

      SumRef   := SumRef + Refer;
      SumRefsq := SumRefsq + refer*refer;

      inc(n);

    if keypressed then ch:=break;
    if ch='q'then
       begin
       message(msgx,msgy,'Skip this measurement? y/n');
       repeat
         ch:=break;
         if ch='y' then i:=Avnum;
```

```
        until ch in ['y','n'];
        end;

      END;

    Hessage(HsgX,HsgY,'');
    End Else begin
             Hessage(HsgX,HsgY,'Warning!! Persisting overload condition on lock-in.');
             end;

{---omrekeningen-------}

    x.is(sumx/n,sqrt(sumxsq/n - sqr(sumx/n))/sqrt(n-1) );
    y.is(sumy/n,sqrt(sumysq/n - sqr(sumy/n))/sqrt(n-1) );

               {/\ standaard deviatie in het gemiddelde (vandaar / sqrt(n))
                we berekenen SDn-1 vandaar /sqrt(n-1)
               }

    lijst.init;
    lijst.voegtoe(@x);
    lijst.voegtoe(@y);
    totphase:= eval2(hoek,lijst)^.scalp(1/Pi*180)^; {phase in graden}
    lijst.disposelijst;

    sig := mpsqrt(mpsqr(x)^.plus(mpsqr(y)^)^)^;

    refout := mp(SumRef/n,sqrt(sumrefsq/n-sqr(sumref/n))/sqrt(n-1) )^.min(refzero)^;

    lijst.init;lijst.voegtoe(@sig);lijst.voegtoe(@totphase);lijst.voegtoe(@sigzero);lijst.voegtoe(@phasezero);
    sigout := eval2(lengteverschil,lijst)^;
    lijst.disposelijst;

    phaseout:=totphase;

  GoToXY(xpos,ypos);
END;       { HeasPhotoCurrent}

{------meting van de achtergrond---------------------------------------}

PROCEDURE DetZero;
BEGIN
  sigzero.is(0,0);
  phasezero.is(0,0);
  refzero.is(0,0);
  message(msgx,msgy,'Determining zero..');
  mulfac:=2*mulfac;
  HeasPhotoCurrent(sigzero,phasezero,refzero);
  mulfac:=mulfac div 2;
  logout('detzero:'+sigzero.mpstr+' '+phasezero.mpstr+'  '+refzero.mpstr);
END;      { DetZero }

{------bepaling Quantum Yield-------------------------------------------}

function QYfun(sig,ref:meetpunt;wavlennum:integer):mppointer;
var caldet:meetpunt;
BEGIN

  IF GeDet THEN CalDet := CalGe[WavLenNum]
                        ELSE CalDet := CalSi[WavLenNum];
  if ref.w<>0 then
  fwaarde[findex]:=mpabs( Sig.maal(CalDet)^.
                          maal(Eph(wavelen[wavlennum])^)^.
                          door(Ref)^.
                          door(Trans[WavLenNum])^.
                          scalp(ConFac)^
                        )^
  else fwaarde[findex].is(0,0);

  QYfun:=@fwaarde[findex];
  inc(findex); findex:=findex mod (maxfunctie+1)

END;      { CalcQY }

procedure measQY(wavnum:integer;var QY,phase,reference:meetpunt);
var sig,ref,ph:meetpunt;
  begin
  HeasPhotoCurrent(sig,ph,ref);
  QY:=QYfun(sig,ref,wavnum)^;
  phase:=ph;
  reference:=ref;
  end;
{----------Hain program-----------------------------------}
....omitted......
```

Appendix C

List of Symbols

The most important used symbols are given in the tabular below. The units used in this report are those from the S.I. rationalized MKSA system. The dimensionality of a quantity follows from the context, and is not indicated with arrows, bold-facing or otherwise.

Symbol	Description	(magnitude) Unit
$A^\star$	Richardson constant	$\approx 1.20 \cdot 10^6$ A/m^2/K^2
d	thickness of the polymer film	m (nm)
e	absolute charge of an electron	$1.6 \cdot 10^{-19}$ C
e	$\Sigma_{n=0}^{\infty} \frac{1}{n!}$	–
e_p	constant correlated to trap depth and	
	the attempt to escape frequency ν_p	/s
E	energy of an electron	J or eV
E_t	trap depth	J or eV
ϵ	Permittivity of a polymer	$\approx 3\epsilon_0$
ϵ_0	Permittivity of free space	$\frac{1}{(4\pi \cdot 10^{-7}\text{H/m})c^2}$ =$8.84 \cdot 10^{-12}$ F/m
F_{image}	Image force	N
Φ	Work-function of a metal	V
Φ_{barrier}	Potential barrier on a insulator/metal interface	V
h	Planck's constant	$6.62618 \cdot 10^{-34}$ Js
i	current	A
j	current density	A/m^2
k_B	Boltzmann constant	$1.38 \cdot 10^{-23}$ J/K
λ	wavelength of light	m (nm)
m	mass of an electron	$0.91095 \cdot 10^{-30}$ kg
$m^\star$	effective mass of an electron ($\approx m$)	kg
μ	microscopic mobility of a carrier in polymer	m^2/Vs
μ_0	microscopic mobility at zero field in polymer	($\approx 10^{-10}$) m^2/Vs
n	free electron density	electrons/m^3
n_t	trapped electron density	electrons/m^3
N_C	density of states in conduction band	states/m^3
N_V	density of states in valence band	states/m^3
N_t	traps density	trap states/m^3

p	free hole density	holes/m^3
p	momentum of an electron	kg m / s
p_t	trapped hole density	holes/m^3
q	charge of an electron, see e	
T	Temperature	(≈ 300) K
θ	Angle the velocity of an electron with the normal of interface	–
V	voltage	V
χ	Electron affinity of a polymer	V
Y	Quantum Yield	electrons/photon
X_e	quantity associated to electrons (e.g. μ_e)	–
X_h	quantity associated to holes	–
$\int dx$	operator which integrates to x	–
∂_x	operator which differentiates to x	–
()	indicates alternative priority of operators	
()	argument of a function	

List of Figures

Index